

A peer-reviewed version of this preprint was published in PeerJ on 29 June 2016.

[View the peer-reviewed version](https://peerj.com/articles/2176) (peerj.com/articles/2176), which is the preferred citable publication unless you specifically need to cite this preprint.

Pantziarka P. 2016. Emergent properties of a computational model of tumour growth. PeerJ 4:e2176 <https://doi.org/10.7717/peerj.2176>

Emergent properties of a non-physiological computational model of tumour growth

Pan Pantziarka

NEATG is a simple non-physiological tumour growth model which displays emergent properties which are analogous to a number of characteristics common to physical tumour growth. NEATG employs a novel dual-scale evolutionary algorithm which models both cell-autonomous and non-cell autonomous behaviours. The components of the model are outlined briefly, with reference to the core algorithm and data structures. Experimental results are presented which illustrate the behaviour of the model under different evolutionary scenarios, including homeostasis, tumour growth and a number of anti-tumour interventions. In particular the system is used to explore the impact of cytotoxic interventions, (analogous to high-dose chemotherapy), with respect to adaptive responses and evolutionary change. Finally, a number of avenues for further development of the system are discussed.

1 **Emergent Properties of a Non-physiological Computational Model of**
2 **Tumour Growth**

3 Pan Pantziarka^{1,2}

4 ¹ The George Pantziarka TP53 Trust, London KT1 2JP, UK

5 ²Anticancer Fund, Brussels, 1853 Strombeek-Bever, Belgium

6 Email Address: Pan Pantziarka: anticancer.org.uk@gmail.com

7 Abstract

8 While there have been enormous advances in our understanding of the genetic drivers and
9 molecular pathways involved in cancer in recent decades, there also remain key areas of dispute
10 with respect to fundamental theories of cancer. The accumulation of vast new datasets from
11 genomics and other fields, in addition to detailed descriptions of molecular pathways, cloud the
12 issues and lead to ever greater complexity. One strategy in dealing with such complexity is to
13 develop thought experiments which selectively focus on different levels of abstraction in order to
14 build models to replicate salient features of the system and therefore to build hypotheses which
15 reflect on the real system. NEATG is a simple non-physiological tumour growth model which
16 displays emergent behaviours that correspond to a number of clinically relevant phenomena
17 including tumour growth, intra-tumour heterogeneity, growth arrest and accelerated repopulation
18 following cytotoxic insult. Analysis of model data suggests that the processes of cell competition
19 and apoptosis are key drivers of these emergent behaviours. Questions are raised as to the role of
20 cell competition and cell death in physical cancer growth and the relevance these have to cancer
21 research in general is discussed.

22 Introduction

23 Tumour growth is a complex process characterised by multi-scale phenomena involving both
24 cancer and non-cancer cell populations. Where previously our focus was directed primarily at the
25 activities of the cancer cell populations, once conceptualised as a single homogeneous mass, our
26 increased understanding of cancer biology now incorporates a more nuanced evolutionary or
27 ecological view of cancer growth (Gatenby, Gillies & Brown, 2011; Kareva, 2011). Key
28 elements of this view of cancer as an evolutionary system are a focus on the genetic
29 heterogeneity of tumour cell populations (Fisher, Pusztai & Swanton, 2013; De Sousa E Melo et
30 al., 2013), the importance of the tumour microenvironment and the cross-talk between cancer
31 and non-cancer cell populations (Allen & Louise Jones, 2011; Hanahan & Coussens, 2012; Quail
32 & Joyce, 2013). A concern among some investigators is that in the absence of an evolutionary
33 understanding of population dynamics in cancer, therapeutic interventions may be doomed to
34 failure (Silva & Gatenby, 2010; Tian et al., 2011; Gillies, Verduzco & Gatenby, 2012). In other
35 cases there is interest in understanding the role of the microenvironment in the process of cancer
36 initiation (Pantziarka, 2015) or the metastatic cascade (Psaila et al., 2007; Barcellos-Hoff, Lyden
37 & Wang, 2013).

38 More fundamentally, there are also competing theoretical views of cancer at the most basic level.
39 The predominant view of cancer – termed the somatic mutation theory (SMT) – is that it is a
40 disease caused, and then driven, by genetic mutations in cells. An alternative view – termed the
41 tissue-organisation field theory (TOFT) – views cancer as a disease caused by tissue dysfunction,
42 development gone astray, with genetic changes not as the drivers but as a consequence of the
43 disease. A number of recent publications outline these competing views of cancer (Baker, 2014;
44 Bizzarri & Cucina, 2014; Sonnenschein et al., 2014).

45 A challenge to all fundamental theories of cancer is to incorporate the vast array of new data that
46 molecular biology has afforded to the researcher. The literature expands exponentially as we
47 develop the tools to probe ever deeper into cellular structures, signalling pathways and the large
48 data volumes generated by the various ‘omics. Against this backdrop of ever greater detail it is
49 becoming harder to integrate the data into a coherent ‘big picture’. Robert Weinberg makes the
50 point that we are going full circle – from an initially complex picture of disjointed

51 phenomenological facts to simplifying models arising from the revolution in molecular biology
52 and back to a picture of endless complexity again (Weinberg, 2014). The impacts of this lack of
53 progress are ultimately felt in the clinic, where, with a few significant exceptions, progress in
54 developing treatments has significantly slowed in recent years (Jalali, Mitra & Badwe, 2016).

55 Traditionally one tool to aid in the development of theories of complex phenomena is the
56 ‘thought experiment’, a conceptual device with a long and honourable history in the field of
57 scientific investigation. One appealing aspect of a thought experiment is the ability to selectively
58 focus on different levels of abstraction and to selectively ignore those entities or levels of detail
59 which add nothing to the experiment. In so doing one is able to build a model which captures, to
60 a greater or lesser extent, the salient features or the behaviour of the system or object being
61 explored.

62 In more modern guise software allows us to construct simulation models which we can use to
63 construct thought experiments involving complex adaptive systems such as ecosystems, markets
64 and cancer. Such computational models can provide ideal platforms for developing conceptual
65 understanding of complex biological systems (Saetzler, Sonnenschein & Soto, 2011; Janes &
66 Lauffenburger, 2013). A range of techniques are available to build such software models of
67 cancer growth specifically to explore evolutionary or ecological hypotheses at an abstract and
68 non-physiological level, including techniques from evolutionary game theory (Basanta et al.,
69 2008; Krzeslak & Swierniak, 2014) and machine learning (Gerlee, Basanta & Anderson, 2011).

70 Clearly simulation models can vary considerably in scope and intention, particularly with regards
71 to the degree of biological verisimilitude that they undertake to model. Where some models aim
72 to achieve a significant level of physiological accuracy the approach adopted in this work is
73 deliberately non-physiological. As a thought experiment the intention is to build a model using a
74 *minimal* set of objects, properties and behaviours that interact in a manner that is able to
75 reproduce key aspects of tumour growth. This approach is primarily *qualitative* rather than
76 *quantitative* and does not depend on calibration to physical tumour growth models.

77 In contrast many of the computational models that have been developed to date have more
78 clearly defined operational aims. For example Ribba et al created a hybrid cellular automaton
79 model which aimed to replicate some features of CHOP therapy for Non-Hodgkin’s Lymphoma
80 (NHL) (Ribba et al., 2004). The model was calibrated in such a way as to make specific
81 predictions as to the response of NHL cells to treatment with the chemotherapeutic drug
82 doxorubicin. Gerlee and Anderson developed an evolutionary hybrid cellular automaton model
83 of solid tumour growth to investigate the impact of tissue oxygen concentration on the growth
84 and evolutionary dynamics of a tumour (Gerlee & Anderson, 2007). A key aspect of this model
85 was the calibration of parameters with physically relevant data in terms of oxygen and glucose
86 consumption rates, time estimates for cellular proliferation and so on. Enderling and colleagues
87 have developed a series of hybrid cellular automaton models which include both qualitative and
88 quantitative results related to cancer stem cell theory and tumour growth (Enderling, Hlatky &
89 Hahnfeldt, 2009; Enderling & Hahnfeldt, 2011; Poleszczuk & Enderling, 2016). Closer in intent
90 to this work was the genetic algorithm model developed by Gerlee et al to investigate the
91 evolution of homeostatic tissue in a two-dimensional monolayer system (Gerlee, Basanta &
92 Anderson, 2011).

93 NEATG (Non-physiological Evolutionary Algorithm for Tumour Growth) is a simple software
94 model of tumour growth which models cell-to-cell and tissue-level interactions and population
95 dynamics under different evolutionary scenarios. Furthermore the platform is structured such that
96 anti-tumour interventions can also be modelled within these different scenarios. A number of
97 scenarios are explored in this paper, including the simulation of cellular response to homeostasis,
98 stress conditions, nutrient deprivation and cytotoxic intervention.

99 The value of such a modelling approach lies not in the success or otherwise of the model outputs
100 (the emergent behaviour of a modelled tumour mass), but in what objects, properties and
101 behaviours have to be incorporated into the model to produce the desired outcomes. In so doing
102 we may reflect on the actual biological actors and mechanisms which are being modelled and
103 therefore generate biologically plausible hypotheses to be tested in the real laboratory. In this
104 way, perhaps, we may be able to focus on what is important for the development of fundamental
105 theories of cancer, including the SMT and TOFT theories, and also to direct us as to what we can
106 put aside from that ever growing mountain of detailed data.

107 While computational models enable the construction of thought experiments involving biological
108 systems, they differ from traditional mathematical models (differential and other equation-based
109 systems) in that the model itself is encoded in computer code, input/output file formats,
110 configuration files etc. They are, in a very real sense, 'opaque' (Paolo et al., 2000). Therefore, it
111 is important in reporting on such a model that there is exposition not just of the algorithmic
112 details but also an exploration of how the model behaves at different stages, of results with
113 differing inputs, the modelling of different scenarios and so on. Therefore the Results section of
114 this work presents a significant level of detail in the hope that we can lessen the degree of
115 opacity.

116 **Methods**

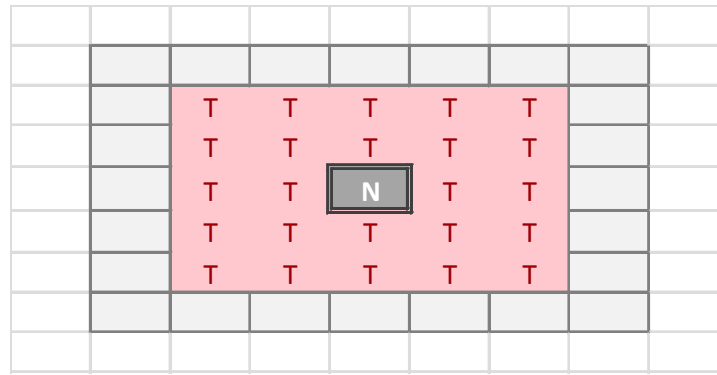
117 NEATG is implemented as a hybrid model incorporating elements from both genetic algorithms
118 and cellular automata. It is dual scale, non-deterministic and represents both cell-level and tissue-
119 level behaviour. It is coded in the Java programming language.

120 **Grid or Tissue-Level**

121 The tissue-level is represented as a rectangular grid, with each grid element containing a set of
122 modelled cells, which may be Malignant or Normal. The relative proportion of Normal and
123 Malignant cells in a grid element determines the state of that grid element. These states are:

$$124 \quad E = \{\text{Normal, Majority Normal, Majority Malignant, Tumour, Necrotic}\}$$

125 Transition of a grid element from one state to another takes place at every clock tick and is
126 determined by the proportions of different cell populations within that element, but also by the
127 state of neighbouring grid elements. Grid elements which are in the Tumour state, that is they do
128 not have any Normal cells within them, can transition to a Necrotic state if they are surrounded
129 by an extended neighbourhood which consists exclusively of other Tumour grid elements. By
130 default this is a Moore neighbourhood of radius 2 (see Figure 1), though this is a configurable
131 model parameter.



132

133

Figure 1 - Moore Neighbourhood of radius 2

134 Grid elements in the Necrotic state are suspended and do not take part in further computational
 135 activity unless the neighbouring grid population changes, in which case the Necrotic state reverts
 136 to Tumour.

137 Each grid element is populated with an initial, optimum population of Normal cells. The size of
 138 this optimum population is a model parameter that can be varied. The size of the population can
 139 vary over time and can increase to a defined maximum value after which cellular competition
 140 takes place (as described below).

141 Each grid element receives as input a Nutrient, represented as an integer value, and a set of Gene
 142 Factors, represented as real values. The number of Gene Factors is equal to the number of genes
 143 in the cell structure, again this is a model parameter that can vary, but the default number is 3.
 144 The Nutrient score can be loosely interpreted as a combination of oxygen and cellular nutrients
 145 (e.g. glucose), while the Gene Factors may be viewed as generic growth factors required for
 146 cellular growth and survival.

147 The grid element has a distribution function to compute the share of Nutrient (DN) assigned to
 148 each cell in its population of P cells based on the relative demand represented by the Nutrient
 149 Target values T for each cell:

150

$$DN_i = \frac{T_i}{\sum_{p=1}^P T_p}$$

151 Similarly the Gene Factor values which are inputs into each grid element are distributed to each
 152 cell according to the transfer function based on the Gene Targets (G):

153

$$DG_i = \frac{G_i}{\sum_{p=1}^P G_p}$$

154

155 **Cell Level**

156 There are two types of cell in this model, Normal and Malignant, with the same internal structure
 157 regardless of type. While the structure is the same the behaviour is type-dependent during cell
 158 division, as will be shown later.

159 Each cell is a data structure that encodes a Genome and an internal clock. The internal clock,
 160 implemented as an integer value, counts down from a maximum value, known as the Lifetime, to
 161 zero. Cell division is initiated when the clock reaches zero. When the system is first instantiated
 162 each cell is initialised with an internal clock value that is equal to a random integer between the
 163 Lifetime and zero. The Genome is a set of N genes, which are defined by a Target and a
 164 Tolerance, both represented as real numbers. The Genome is defined as:

$$165 \quad G = \{(Target_0, Gene\ Tolerance_0) \dots (Target_N, Tolerance_N)\}$$

166 The Target is the optimum level of the corresponding Gene Factor that exists in the grid
 167 environment, and the Tolerance defines a band of tolerable values on either side of the Target
 168 that is the healthy range for that gene. Gene health is therefore defined as a Boolean value which
 169 evaluates as True when the Gene Factor is within the desired range, or False if the Gene Factor is
 170 above or below the tolerable range:

$$171 \quad Health = (Gene\ Factor < (Gene\ Target + Gene\ Tolerance)) \ \& \ (Gene\ Factor > (Gene\ Target - \\ 172 \quad Gene\ Tolerance))$$

173 In addition to flagging health status, Genes are also used as a mechanism for the cell to influence
 174 the local grid environment. This is a simple feedback mechanism by which each cell attempts to
 175 alter the local environment in order to achieve the level of Gene Factor required for its own
 176 optimum health. The expression function is:

$$177 \quad E = 1 - e^{-(T - F)}$$

178 Where T is the Gene Target value and F exogenously supplied Factor.

179 The actual level of Gene Factor available in each Grid Element is calculated as the sum of the
 180 exogenously supplied Factor, which is an input parameter in the model, and the sum of the
 181 expression values from each cell in that grid element.

182 Additional components of the cell are the Nutrient Target and a Nutrient Rate, which represent
 183 the demand for nutrient and the rate at which nutrient is consumed respectively. Nutrient which
 184 is not consumed is stored in the Nutrient Store. Each cell also has a Mutation Rate and an
 185 Invasion Rate, which are used when cell division is necessitated for Malignant cells.

186 Cells can exist in a number of states:

$$187 \quad S = \{HEALTHY, DIVIDING, APOPTOTIC, TO_BE_CLEARED, NECROTIC\}$$

188 Note that the cell state of Healthy implies viability, rather than whether a cell is Normal or
 189 Malignant.

190 At every clock tick the health status of each cell is assessed and the cell clock decremented
 191 according to the state of health. A healthy cell, with adequate Nutrient and Gene Factors, will

192 decrease the cell clock by 1. Each unhealthy gene will also decrement the cell clock by one. A
 193 cell that has a value of zero for Nutrient store will have the cell clock set to zero because it is
 194 unable to meet its metabolic requirements and must therefore transition from a Healthy state.

195 All cells undergo a similar cell cycle. A cell starts as Healthy and undergoes a number of
 196 iterations (clock ticks) in which nutrient and gene factors are processed, the cell clock decreases
 197 at rates that depend on how well the cell is adapted to the local grid environment defined by the
 198 available Nutrient and Gene Factors. When the cell clock or nutrient store reaches zero the cell
 199 changes state according to the following cycle:

200 Healthy > Dividing > Apoptotic > To Be Cleared

201 Cells that are flagged as To Be Cleared are removed from the grid element. Dividing cells
 202 undergo cell division during which a new daughter cell is generated and enters the local
 203 population. When the grid element contains fewer than the maximum number of supported cells
 204 (termed the carrying capacity of the grid element) a new cell is cloned from the dividing cell. In
 205 the case of Malignant cells this cloning can also incur a mutation in which one of the elements of
 206 the cell can change value, for example the Nutrient Target, a Gene Tolerance value or the cell
 207 Lifetime itself may undergo an increase or decrease. Note that the rate of mutation events is
 208 controlled by the Mutation Rate, which is itself mutable and can increase or decrease.

209 If the grid element is already supporting the maximum number of cells then the cell division
 210 process is more complex. In addition to undergoing a chance of mutation, Malignant cells may
 211 also undergo a migration event in which the cell moves into a randomly selected adjacent grid
 212 element. The rate of such migration events is controlled by the Invasion Rate, which, like the
 213 Mutation Rate, is mutable. Cells which are not selected for migration are added to the local
 214 population. To preserve the carrying capacity of the grid element, all cells are then ranked
 215 according to fitness and the least fit cells are removed. This ranked selection algorithm is not
 216 biased by cell type, and both Malignant and Normal cells are included in the process.

217 The fitness function, F , is designed to penalise cells which are poorly adapted to the *local* grid
 218 environment rather than being a global function across the entire population of cells. It is defined
 219 as:

$$220 \quad F = \sum_{g=1}^G e^{-\left(\frac{|T_g - A_g|}{T_g}\right)}$$

221 where T is the Gene Target and A is the Gene Factor value for each Gene in the Genome G .

222 Evolutionary Strategies

223 The processing of Nutrient and Gene Factors is controlled by the treatment strategy object active
 224 during that clock tick. This software component, coded in Java, enables the NEATG system to
 225 model multiple evolutionary strategies, each of which can implement different algorithms in
 226 terms of controlling the rate of cellular attrition, ageing and division. For example it is possible
 227 to implement a strategy which mimics high-dose chemotherapy and stops dividing cells from
 228 successfully completing the replication process. Alternatively a treatment strategy may alter the
 229 nutrient supply to mimic starvation or over-feeding.

230 Treatment strategies become active at specific time points, either by activation at a specified
231 iteration or at a specified level of tumour growth. Once triggered a treatment strategy can remain
232 active until the final iteration or for a specified number of iterations. There is also a default ‘no
233 treatment’ strategy during the iterations before and after the ‘active’ strategy is in operation.

234 **Run-time Behaviour**

235 The run-time behaviour of NEATG is specified using a scenario file which sets the key
236 parameters for both the structure of the grid and the cell populations. Initial parameters include
237 the dimensions of the grid, optimum and maximum cell counts for grid elements, the number of
238 iterations or clock-ticks, the name of the active strategy and the trigger point and duration of
239 action. In terms of cell structure the key parameters include the number of genes, the gene
240 structure, the mutation and invasion rates and the lifetime of each cell. Another key input to the
241 system is the structure of the Malignant cell, both in terms of the gene structure but also in terms
242 of the number of malignant cells to insert into the system and at which iteration they should be
243 inserted.

244 There are numerous logging, statistics and output generation features implemented by the
245 system, and these too are controlled via the scenario file. As the system is non-deterministic and
246 displays considerable variation in behaviour depending on the evolutionary processes of
247 mutation and invasion, an additional scripting mechanism is implemented so that multiple runs
248 can be performed and the data stored together for later analysis and reporting.

249 **Results**

250 **Homeostasis**

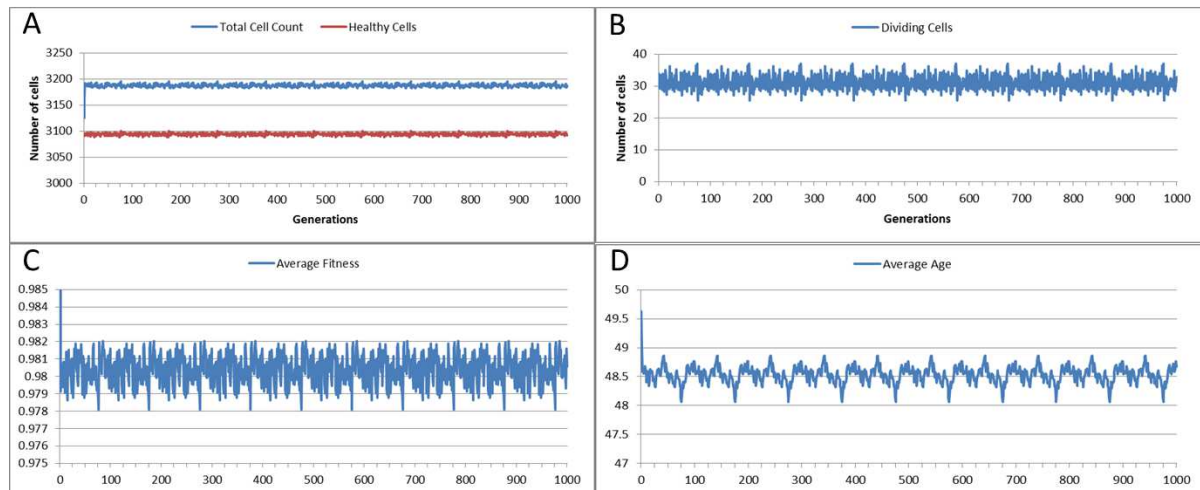
251 Before exploring the results for different tumour growth scenarios it is important to validate the
252 behaviour of the system during homeostatic and non-tumour scenarios. Cells in this scenario are
253 supplied with optimal Nutrient and Gene Factor values, ensuring that they are unstressed and in
254 ‘good health’. In the absence of tumour cells we would expect that the system will display
255 homeostatic behaviour characterised by regular cellular turn-over as cells age and die, and that
256 cell population size will fluctuate but remain relatively constant.

257 To represent this scenario a series of experiments were run using a 25 x 25 grid. The optimum
258 cell population for each grid was set at 5, with a population of 10 cells as the maximum carrying
259 capacity. The Nutrient Target used was 10, with a Nutrient Rate of 1. The Nutrient input to each
260 grid element was also set at 10, ensuring that at optimum population level each cell would
261 receive a Nutrient input of $10 / 5 = 2$. A genome of three identical genes was used:

$$262 \quad G = \{(5.0, 1.0), (5.0, 1.0), (5.0, 1.0)\}$$

263 The Gene Factor supplied to each grid element was set at $\{25.0, 25.0, 25.0\}$, to ensure that each
264 cell received the Target value of 5.0.

265 The system was run five times, with 1000 iterations per run, and the results averaged for this
266 analysis. Given our input parameters for a grid of 625 elements (25 x 25), and an optimum cell
267 density of 5 cells per grid element, we would expect a total cell count of 3125. However, not all
268 of these cells will be healthy, some will be dividing or being cleared. Figure 2A shows the
269 overall population of cells over time.



A. Total and healthy cell counts over time. B. Number of dividing cells over time. C. Average cell fitness over time. D. Average cell age over time.

270

271 **Figure 2 - Cell change over time**

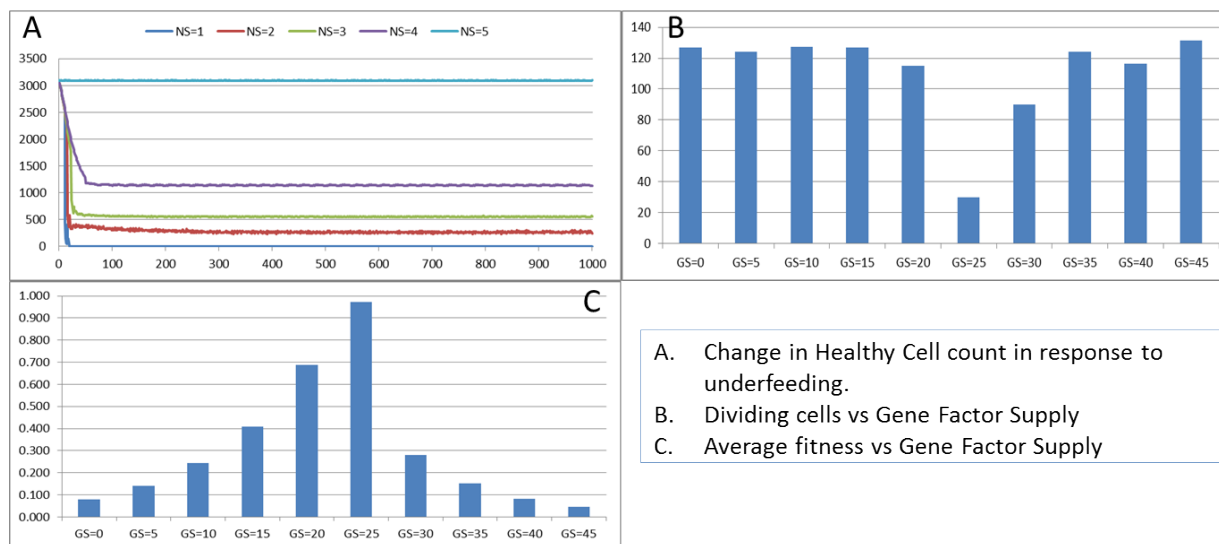
272 The number of dividing cells over time is shown in Figure 2B. Note that the average over the
 273 1000 iterations is 31.25. This is as we would expect given that the Lifetime for the cells is 100,
 274 so that at any one time 1% of cells is dividing.

275 The average fitness, Figure 2C, is high, fluctuating just below the maximum possible value of
 276 1.0. And the average age, Figure 2D, fluctuates just below a value of 50. These latter two figures
 277 display more clearly a pronounced periodicity which is also evident in the population density.
 278 This is due to the random distribution of ages in the initial cell population. In the absence of
 279 stress or environmental perturbation the population of cells ages and divides in a uniform manner
 280 that preserves the distribution of ages from the initial population.

281 **Stress Conditions**

282 In the next experiments we assess the behaviour of NEATG when homeostasis is disturbed. In
 283 particular we are interested in the responses to changes in Nutrient and Gene Factors as these
 284 both have an influence on cell ageing and survival. Again this series of experiments does not
 285 include Malignant cells as we are primarily interested in exploring the behaviour of the system in
 286 non-tumour scenarios. For both of the following experiments the same basic parameters as in the
 287 previous experiment are used.

288 The first stress experiment varies the Nutrient input from 1 to 15, in integer steps. Given that the
 289 Nutrient Rate is set at a value of 1 and the optimum cell population is set to 5, we would expect
 290 that if the Nutrient Supply to each grid element falls below a value of 5 each cell in the grid
 291 would consume more nutrient than it receives as input and eventually deplete the value in its
 292 Nutrient Store (which was set to an initial value of 10). Figure 3A shows the number of healthy
 293 cells for different Nutrient Supply values. There is a decline in cell numbers over time for
 294 Nutrient Supply values below 5 but none for greater values (data not shown). Cell populations
 295 are therefore shown to be sensitive to the supply of Nutrient such that under-feeding can deplete
 296 numbers and in some cases 'starvation' reduces cell numbers to zero.



297

298 **Figure 3 - Changes during Stress Conditions**

299 The supply of Gene Factors is the other external input to each grid element. These are analogous
 300 to generic growth and survival factors and are used to assess the health or otherwise of each cell
 301 in a grid element. In this experiment the same parameters are used as before, but the Gene Factor
 302 Supply is varied from {0.0, 0.0, 0.0} to {45.0, 45.0, 45.0}, in increments of 5.0.

303 There was little variation in cell counts in response to changes in Gene Factor Supply (data not
 304 shown), however, Gene Factors did have an influence on cell turnover, such that it was lowest
 305 for optimum values of Gene Factor Supply and increased by a factor of four as the deviations
 306 from the optimum values increased, as shown in Figure 3B. The number of dividing cells at the
 307 optimal Gene Factor Supply value is around 1% of the total cell count, whereas for non-optimal
 308 Supply values there is an increased rate of cell division. This is as we would expect given that
 309 ‘unhealthy’ genes cause an increased rate of cell aging.

310 In addition to being a factor in the cellular aging process, the Genes are also used in calculations
 311 of cell fitness. Fitness is used in the rank selection process to identify the least fit cells when the
 312 population density in a grid element exceeds the maximum capacity. In this experiment no
 313 Malignant cells are present therefore the rank selection procedure is not active; however we can
 314 still assess the influence of the Gene Factor Supply on cell fitness, (which is defined in the range
 315 [0, 1]), as shown in Figure 3C.

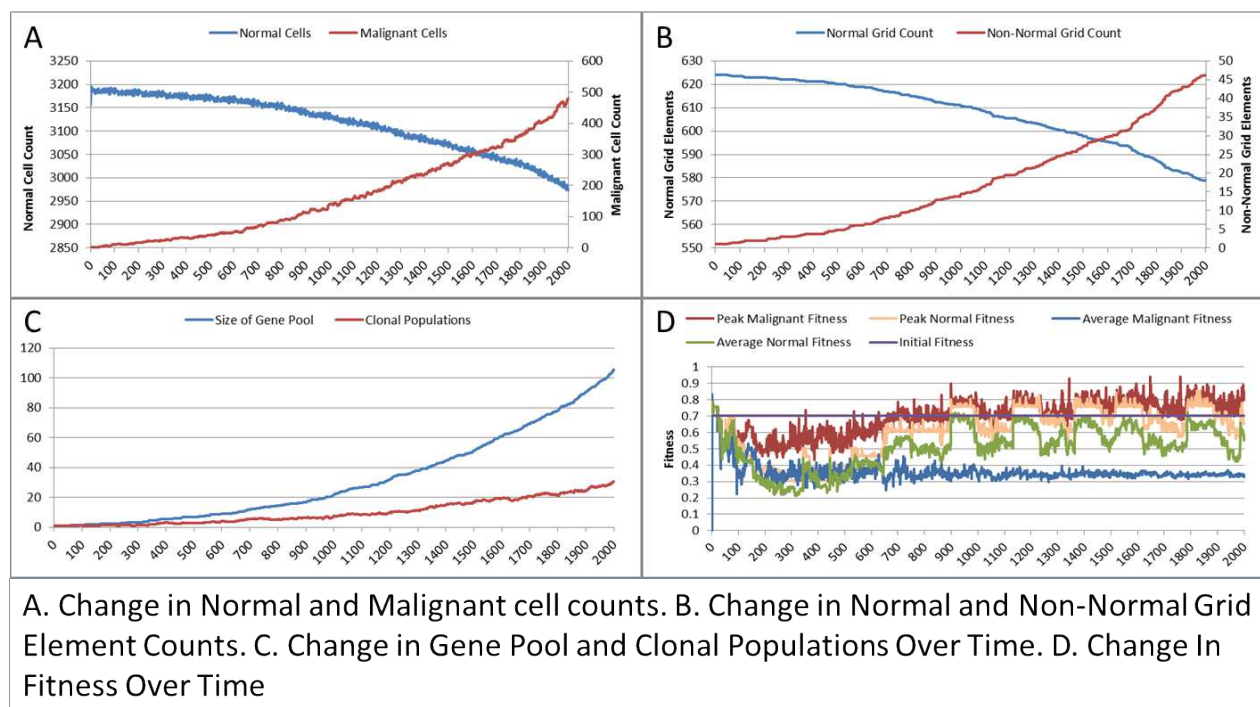
316 **Tumour Growth - No Treatment**

317 Having established the behaviour of the system under homeostatic and non-tumour stress
 318 scenarios, we can now begin to introduce Malignant cells. Initially we will explore the behaviour
 319 of NEATG in the absence of any treatment scenarios.

320 In this first series of experiments we will continue to use the same parameters as before, although
 321 the iteration period is increased to 2000 to allow greater time for the evolution of appreciable
 322 tumour masses. Tumour growth is initiated by the insertion of a single Malignant cell into the
 323 grid element in the centre of our 25 x 25 grid. The only difference between this Malignant cell
 324 and the Normal cells is that the cell type is set to Malignant, and that it has a mutation rate of 5%

325 and an invasion rate of 10%. These initial values were derived from empirical testing of NEATG
 326 and were selected as they generated consistent tumour growth. In subsequent experiments these
 327 values will be varied so that we can see how tumour growth patterns are affected.

328 With the introduction of Malignant cells we can view results both in terms of the changes in cell
 329 populations across the whole system and also in the evolution of the grid elements. The change
 330 in the global population counts cells is shown in Figure 4A and grid elements in Figure 4B.



331

332 **Figure 4 - Tumour growth - no treatment**

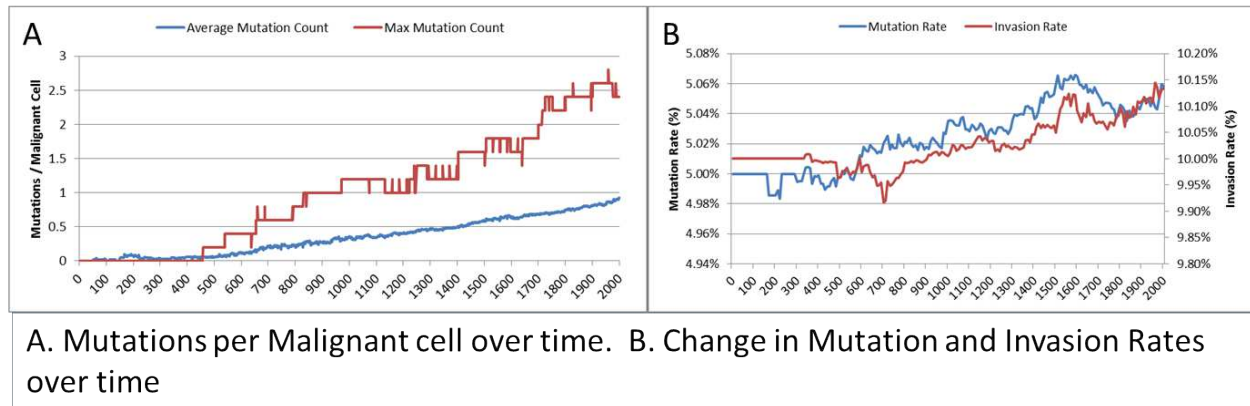
333 Changes in grid elements and cell populations are not the only metrics of interest. Also of
 334 interest is the process of evolutionary change in the Malignant cell populations. In the initial
 335 population there is only a single genotype but as shown in Figure 4C the rate of change of the
 336 gene pool rises over time, increasing in line with the Malignant cell counts. Also shown in Figure
 337 4C is the rise in the number of clonal sub-populations, reflecting the growth of different active
 338 Malignant cell sub-populations in the tumour mass.

339 The evolution of fitness is shown in Figure 4D. The first Malignant cell has the same fitness as
 340 the Normal cells in the grid element into which it is inserted, however as the number of cells
 341 increases, the number of mutations rises, Malignant cells proliferate into neighbouring grid
 342 elements and competition for Nutrient and Gene Factors takes place.

343 The noisy signals indicate a good deal of change and adaptation taking place over time. The
 344 initial high fitness value is degraded once the cell populations start to increase and competition
 345 takes place. It is also clear that the Normal cell population retains an average fitness that is
 346 higher than the average of the Malignant cell population. One plausible explanation is that many
 347 of the mutations are deleterious and do not lead to improved survival for those cells. However, if

348 we look at the maximum values for the Malignant cells we can see that there are indeed some
 349 cells which do achieve a higher fitness than maximum of the Normal cells.

350 The average and maximum number of mutations per Malignant cell, again as a measure of the
 351 degree of evolutionary change, are shown in Figure 5A. As can be seen for the first 100
 352 generations or so there are no mutations, which accords with Figure 4D.

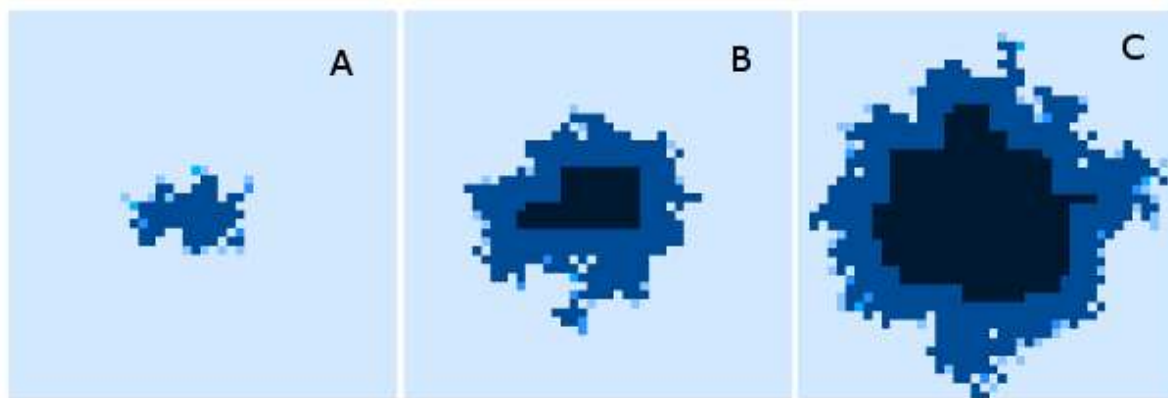


353

354 **Figure 5 - Mutation rates over time**

355 The mutation rate and the invasion rate, which are both mutable characteristics show some
 356 change over time, as shown in Figure 5B. While initially there is little change, indeed both rates
 357 dip below the starting values, both rates show an increasing trend over time.

358 Finally, while we have explored the rates of change at the cellular and grid element levels, we
 359 have not explored the spatial distribution of the spread of Malignant cells. A representative
 360 example of the ‘no treatment’ scenario is shown in Figure 6, an extended run of 6000 generations
 361 and a grid size of 45 x 45 has been used to illustrate more fully the development of the tumour
 362 mass over time.



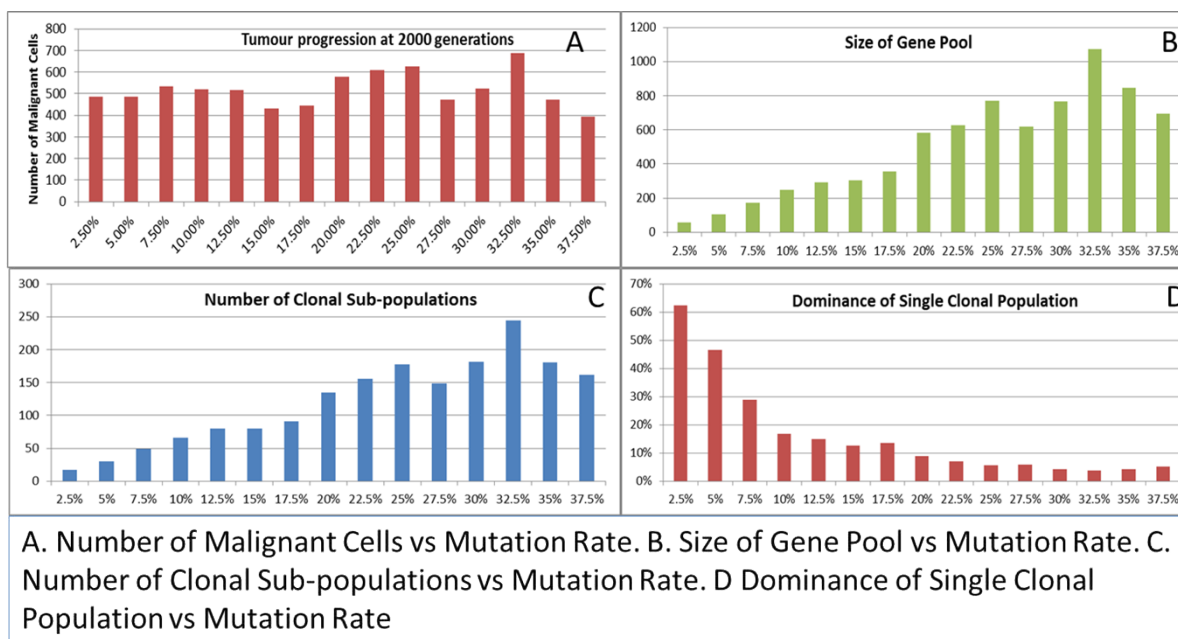
Evolving tumour mass at A: 2000 generations, B: 4000 generations, C: 6000 generations. Note that black areas are necrotic grid elements.

363

364 **Figure 6 - Spatial distribution of tumour growth**

364

365 We can vary the Mutation and Invasion rates to understand the impact they have on tumour
 366 growth. First we vary the Mutation Rate from 2.5% to 30% in increments of 2.5%, all other
 367 settings are as before. Note that while figures are shown for the final time point of 2000
 368 generations, these values are representative of the trends apparent at earlier time points. Whether
 369 we look at tumour progression in terms of grid elements or in terms of Malignant Cell counts, as
 370 in Figure 7A, there is no direct relationship between mutation rate and tumour progression.

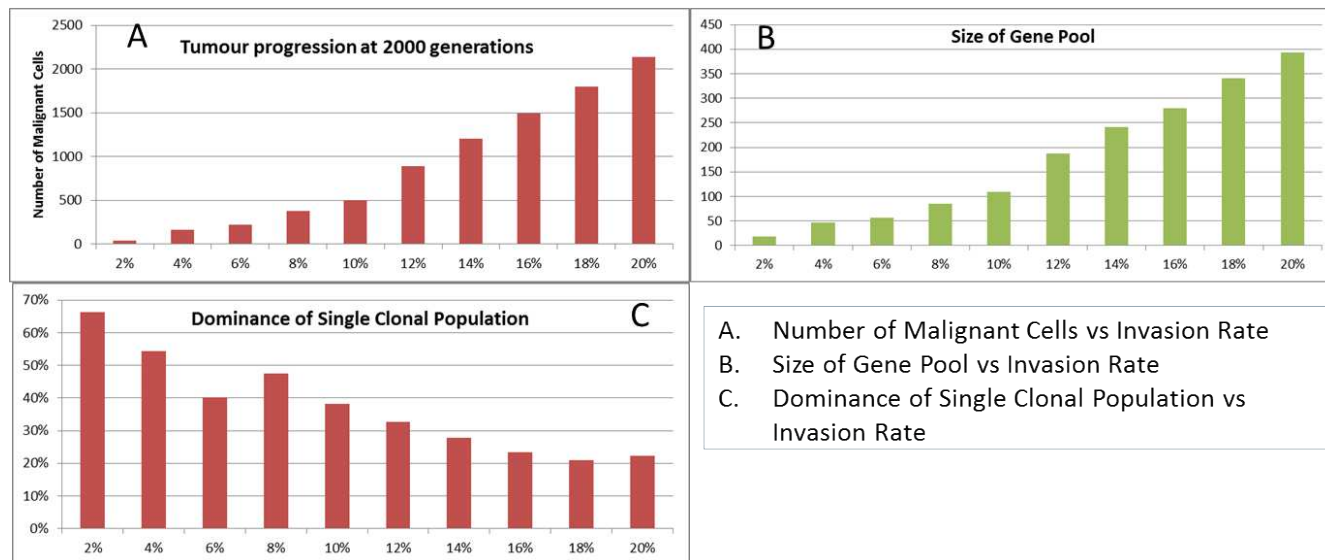


371

372 **Figure 7 - Mutation rates and clonal sub-populations**

373 We would expect to see a correlation between the mutation rate and the size of the Gene Pool,
 374 Figure 7B, though even here the relationship is not completely linear as a mutation rate of 32.5%
 375 generated a larger gene pool than a mutation rate of 37.5%. Similarly, if we look at the number
 376 of clonal sub-populations, Figure 7C, there is a correlation with the mutation rate, but again this
 377 is not linear. Another interesting metric is the degree of dominance of the largest of the clonal
 378 sub-populations, Figure 7D. This shows the percentage of the total number of Malignant cells
 379 which belong to the largest clonal sub-population and shows that a lower mutation rate yields a
 380 greater degree of dominance by a single clonal sub-population.

381 We also vary the Invasion Rate to see what impact this has on the degree of tumour growth and
 382 the size of the gene pool. In this experiment the Invasion Rate is varied from 2% to 20% in 2%
 383 increments, the Mutation Rate of 5% is used; all other settings are as before. Clearly, as shown in
 384 Figure 8A, there is a direct relationship between the Invasion Rate and the rate of tumour growth.
 385 More migration events correlate closely with increased tumour spread.



386

387 **Figure 8 - Invasion rates and clonal sub-populations**

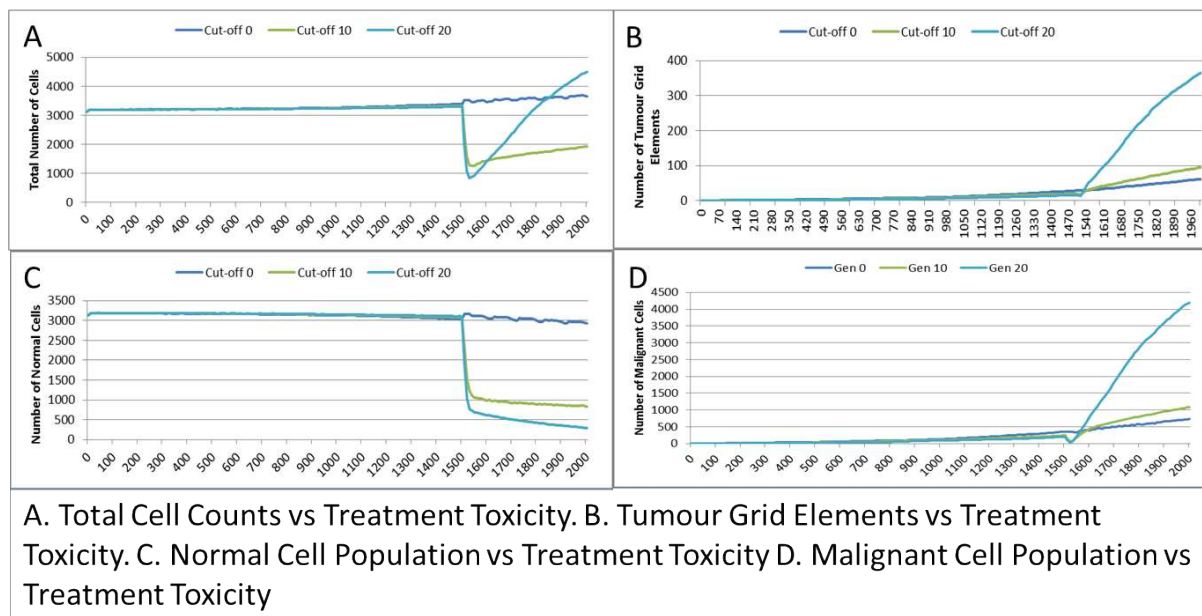
388 This increased rate of tumour growth also leads to an increase in the size of the Gene Pool,
 389 Figure 8B. However, when compared to the scale of the increase of the Gene Pool with a rising
 390 Mutation Rate (Figure 7B) it is clearly lower and indicates a less heterogeneous Malignant cell
 391 population. In terms of the dominance of a single clonal population, Figure 8C, a lower Invasion
 392 rate is associated with an increased dominance by a single clonal sub-population, but even at a
 393 high Invasion Rate of 20% the degree of dominance is much higher than that associated with a
 394 high Mutation Rate (Figure 7D).

395 **Tumour Growth - With Treatment**

396 The previous experiments have shown that in the absence of any interventions the number of
 397 Malignant cells and Tumour grid elements increase over time. In the next series of experiments
 398 we investigate the impact on these growth patterns of a number of interventions using an active
 399 treatment strategy. This is loosely based on the example of high-dose cytotoxic chemotherapy.
 400 Just as with cytotoxic chemotherapy this is not a targeted therapy – it is applied to both Normal
 401 and Malignant cells. Where real chemotherapy causes apoptotic or necrotic cell death in rapidly
 402 dividing cells, the treatment strategy in this model flags cells above a specified age with the cell
 403 state of TO_BE_CLEARED. The arbitrary age cut-off is based on the value of a cell's clock and
 404 this value is a configurable parameter. By adjusting the cut-off value we can approximately
 405 control the 'toxicity' of the treatment, the higher the cut-off value the more toxic the treatment as
 406 more cells will be flagged for disposal. The system also allows a degree of specificity in that we
 407 can make Malignant cells more susceptible to the treatment than Normal cells.

408 In this experiment the same parameters will be used as in the No Treatment scenario. The
 409 treatment will commence at generation 1500 (of 2000), and will be applied for 25 generations.
 410 Three different toxicity values are assessed, with both Malignant and Normal having the same
 411 cut-off values. The values used are 0, 10 and 20, which means that any cell with a clock value \leq
 412 the cut-off is 'treated'. Note that the zero cut-off value does not trigger cell division as in the
 413 default scenario, but triggers apoptosis and cell clearance. It represents the least toxic scenario
 414 and is therefore close to the 'no treatment' scenario.

415 The effect of treatment on the total cell count, Figure 9A, is dramatic. In the case of the more
 416 toxic treatments, there is a sharp decline in total cell numbers followed by a recovery, and in the
 417 case of the highest cut-off value of 20 cell growth accelerates above the pre-treatment trend.

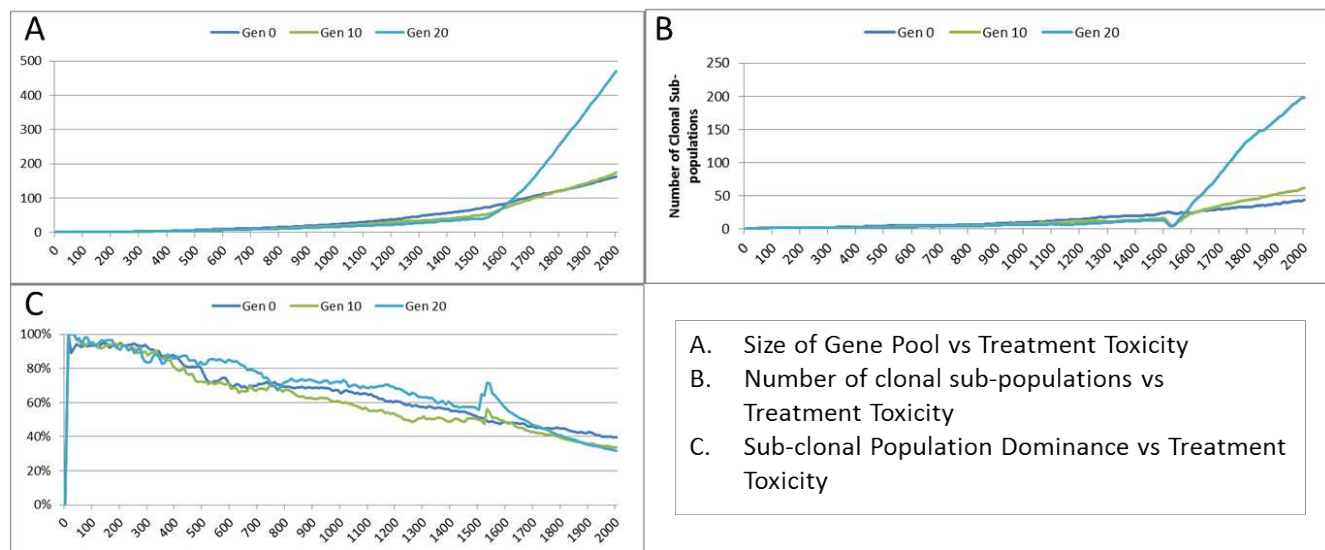


418

419 **Figure 9 - Tumour response to treatment toxicity**

420 This growth trajectory is also reflected in the Grid Element view of tumour growth, Figure 9B.
 421 This shows that the slow rise in number is briefly interrupted when treatment begins but then
 422 accelerates sharply after the completion of treatment. Furthermore in both figures the more
 423 aggressive treatment is related to an increased tumour growth rate following the cessation of
 424 treatment.

425 The change in the Normal Cell population is shown in Figure 9C. The treatment induces a sharp
 426 reduction in cell numbers that continues even after the cessation of treatment, though not at the
 427 same rate. In the case of the Malignant Cells, Figure 9D, there is a decline in cell numbers during
 428 the treatment, followed by rapid recovery. We can assume that the decline in Normal cell
 429 numbers has provided the conditions in which Malignant cells can expand rapidly in number.
 430 Supporting evidence is provided by the Gene Pool trends, shown in Figure 10A. Here we can see
 431 that following treatment there is an increase in the size of the Gene Pool, indicating a post-
 432 treatment burst of clonal evolution.



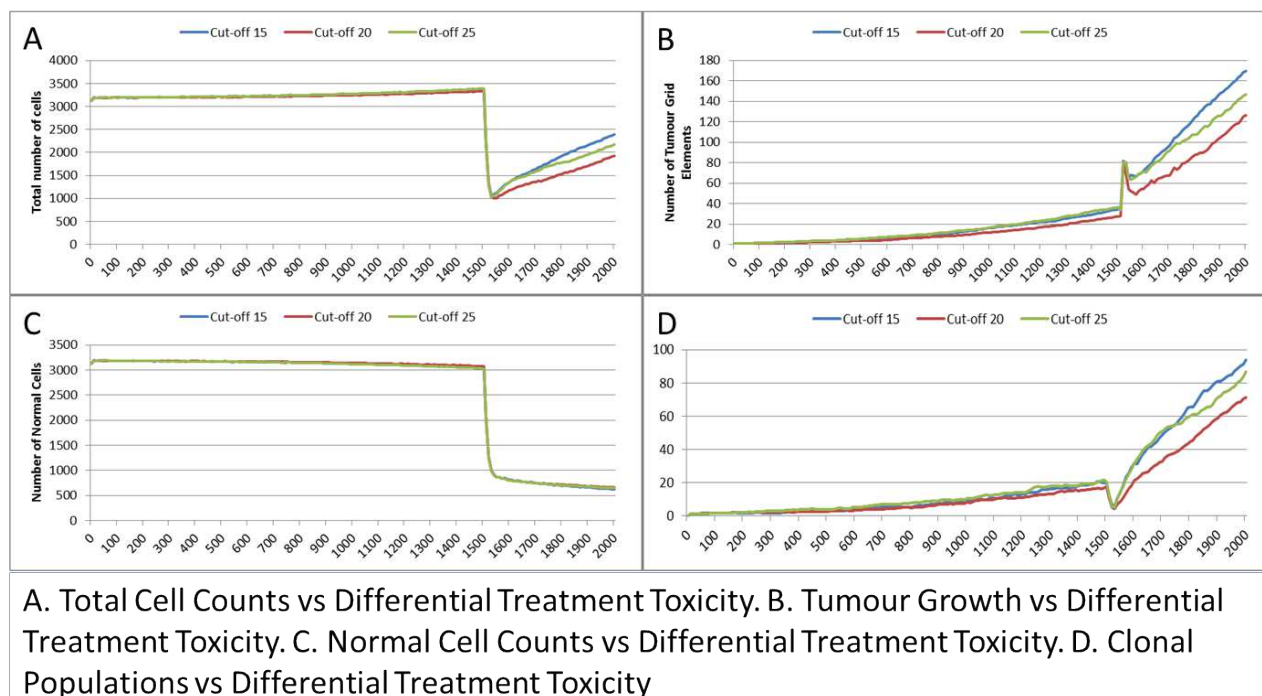
433

434 **Figure 10 - Treatment toxicity and clonal sub-populations**

435 The number of active clonal subpopulations, Figure 10B, shows a similar trend – a slow increase
 436 until treatment commences at which point there is a dip in numbers followed by a post-treatment
 437 evolutionary explosion. Another view of this evolutionary burst, Figure 10C, shows that the
 438 process of tumour growth leads to an increase in genetic heterogeneity, as measured by the
 439 proportion of the Malignant cell population belonging to the largest sub-population. The
 440 increasing heterogeneity is interrupted when treatment begins and there is a spike which shows
 441 that the largest sub-population increases as a proportion of the total, from which we can infer that
 442 a number of clonal sub-populations have been exterminated completely, in line with Figure 10B.

443 In clinical practice maximum tolerated dose (MTD) chemotherapy does not cause equal levels of
 444 damage to all cell populations. Because it impacts rapidly proliferating cells the ‘collateral
 445 damage’ to non-tumour cells is restricted to certain populations of non-cancer cells in the
 446 immune system, gut and other tissues associated with the side effects of treatment (Chen et al.,
 447 2007). We can model this differential impact in the NEATG system by setting a lower cut-off
 448 value for Normal cells compared to Malignant cells, thus causing fewer Normal cells to be
 449 affected. In the following experiment the cut-off for the Normal cells is set to 10, and for the
 450 Malignant cells it is set to 15, 20 and 25 in three different scenarios. All other parameters are the
 451 same as in the previous experiment.

452 In terms of the total cell counts, Figure 11A, there is a similar pattern to the previous experiment,
 453 although the rate of recovery is much lower than in Figure 9A. The picture for grid elements is
 454 shown in Figure 11B. The lower sensitivity of the Normal cells means that even when the cut-off
 455 for the Malignant cells matches the previous values, the recovery of cell populations is lower.



A. Total Cell Counts vs Differential Treatment Toxicity. B. Tumour Growth vs Differential Treatment Toxicity. C. Normal Cell Counts vs Differential Treatment Toxicity. D. Clonal Populations vs Differential Treatment Toxicity

456

457 **Figure 11 - Tumour response to differential treatment toxicity**

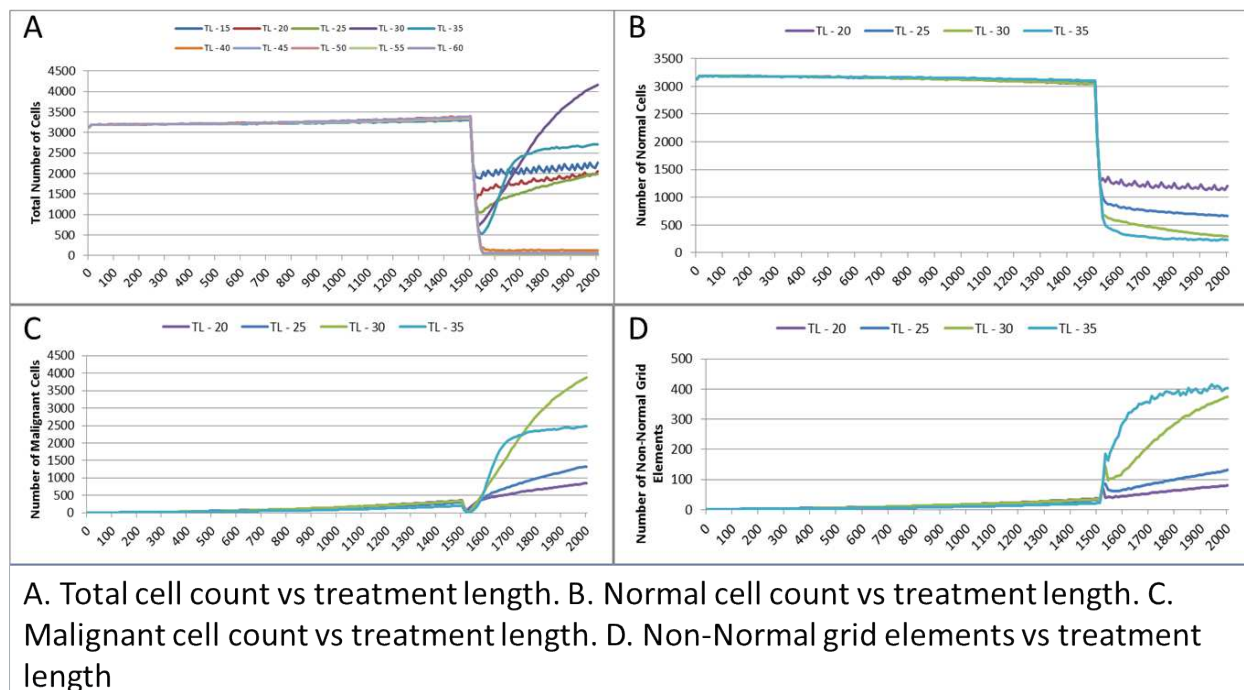
458 The lower sensitivity of the Normal cells does not mean that they are immune from effects of
 459 treatment. Figure 11C shows a marked decline when treatment commences, followed by a
 460 continued decline after treatment ends. Note there is no difference in the three scenarios shown,
 461 indicating that the Normal cells are not affected directly by the higher sensitivity of the
 462 Malignant cells. The values shown here are a close match to those shown for the Cut-off 10
 463 scenario illustrated in Figure 9C. The pattern of increased tumour growth and evolutionary
 464 change following the cessation of treatment also occurs, Figure 11D.

465 Two rather obvious questions arise from this data. The first is what happens if the period of
 466 treatment is extended? It is clear that for the duration of treatment the number of Malignant cells,
 467 tumour grid elements and clonal populations decrease. Is it possible to extend the treatment
 468 period so that the entire Malignant cell population is destroyed? Secondly, it is clear that the
 469 treatment damages Normal cells and that this coincides with increased cancer growth following
 470 the cessation of treatment. Therefore we can ask what happens in the case when the differential
 471 toxicity is such that there is *no* damage to the Normal cells – in other words what would happen
 472 in the case of a ‘magic bullet’ which has toxic effects only on Malignant cells? These questions
 473 are addressed in turn in the next two of experiments.

474 In the following experiment the treatment duration which was varied from 15 – 60 generations,
 475 in increments of 5. A differential toxicity was used, with a Malignant cut-off value of 20 and a
 476 Normal value of 10, all other settings are unchanged.

477 Figure 12A, shows a relationship between the treatment length and the size of the total cell
 478 population. The relationship is complex and non-linear, but it is apparent that treatment duration
 479 longer than 40 generations causes significant reductions in the total population. This result was
 480 robust to repeated runs of the system and there was essentially no difference between results for

481 any treatment length above this level. Furthermore, this upper cut-off figure for treatment length
 482 was related to the length of the cell Lifetime (which is 100 in these experiments). In order to
 483 simplify the exposition, the rest of the results in this experiment will focus on treatment lengths
 484 of 20 – 35.

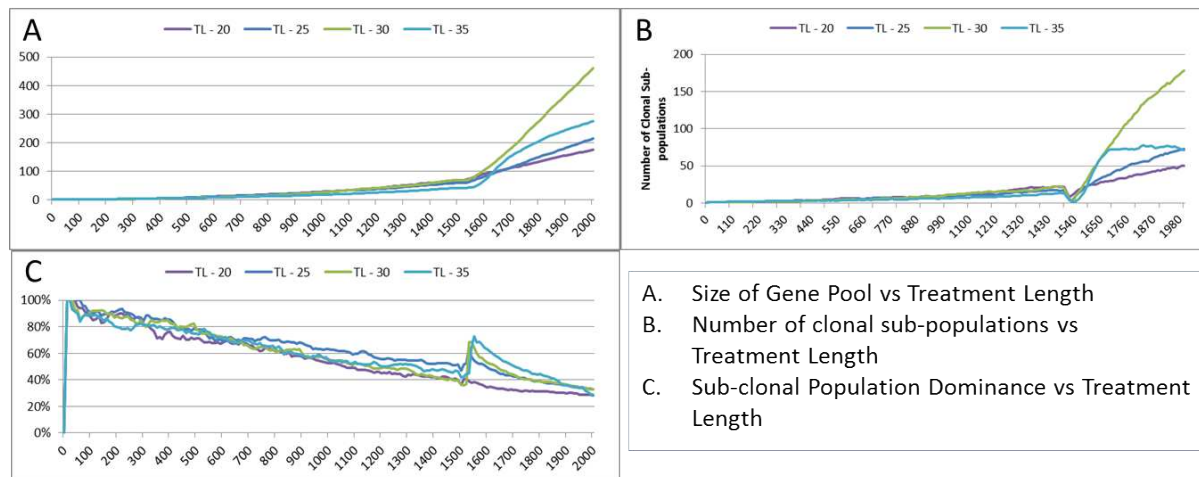


485

486 Figure 12 - Tumour response to treatment length

487 The effect of treatment length on the Normal and Malignant cell populations is shown in Figure
 488 12B and Figure 12C respectively. In the case of the Normal cell populations increasing treatment
 489 length is strongly associated with the scale of the decline in cell numbers. However, in the case
 490 of the Malignant cells, the treatment length is also associated with the rate of recovery. Figure
 491 12C shows that longer treatment length can sometimes lead to an accelerated increase in
 492 Malignant cell numbers, though for treatment lengths beyond 40 (data not shown), there is no
 493 recovery in cell numbers, (as should be clear from the collapse in total cell counts in Figure
 494 12A). The somewhat surprising result is that in some cases a more aggressive treatment (longer
 495 treatment period) can lead to an unexpected acceleration in tumour growth. This is also apparent
 496 in the Grid Element view, Figure 12D, where the post-treatment decline in tumour extent is
 497 followed by a recovery that is related to the treatment length.

498 Length of treatment is also associated with an increase in the size of the Gene Pool, Figure 13A,
 499 and acts as a spur to clonal evolution, as shown in Figure 13B.

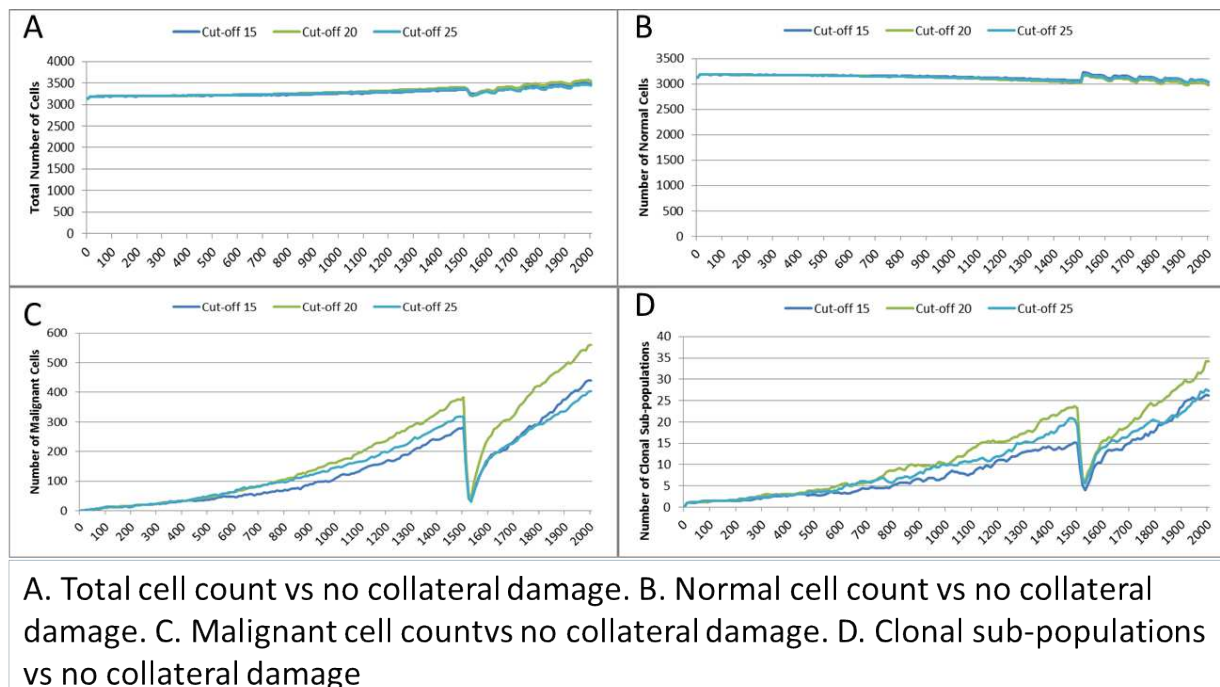


500

501 **Figure 13 - Treatment length and clonal sub-populations**

502 A further indication of the effect of treatment length on clonal evolution is shown in Figure 13C,
 503 which charts the percentage of the total Malignant population in the most populous clonal sub-
 504 population. It is clear that longer treatment increases dominance as cells from less popular
 505 genotypes are removed, whereas for the short treatment of 20 generations there is no such spike
 506 in dominance.

507 In the final experiment in this section we investigate a ‘magic bullet’ scenario where treatment is
 508 applied only to Malignant cells. In this experiment three different toxicity levels are applied to
 509 the Malignant cells, representing cut-off values of 15, 20 and 25. In stark contrast to Figure 9A
 510 and Figure 11A, treatment does not lead to a sharp decline in total cell numbers, as shown in
 511 Figure 14A. This is confirmed by the Normal cell numbers, Figure 14B, where there is a slow
 512 decline prior to the commencement of treatment followed by a recovery in numbers and then a
 513 slow decline again.



514

515 **Figure 14 - Tumour response to no collateral damage**

516 The impact of treatment on Malignant cells, Figure 14C, shows that the increase in cell numbers
 517 is reversed sharply by the treatment but is then followed by a recovery and a resumption of
 518 tumour growth. However, note that while the pattern is similar to previous experiments, the
 519 absolute number of Malignant cells is markedly lower than in Figure 9D and Figure 11D.

520 In terms of the impact on clonal evolution, Figure 14D, while there is a pause during the
 521 treatment period, it continues at a similar rate to the pre-treatment trend afterwards. Again, while
 522 this pattern is familiar, the number of clonal sub-populations is lower than in previous
 523 experiments, as shown by Figure 10B and Figure 13B.

524 Discussion

525 The NEATG model is not a computational model that attempts to emulate the biological
 526 processes involved in tumour growth, indeed it is a very simplistic model that lacks even the bare
 527 essentials of tumour physiology. It does not include any modelling of the immune system, it is
 528 completely avascular, nor does it model specific cell populations. In some respects it may appear
 529 as a simple model of stratified epithelial tissues – the model is partly cellular, the cells are
 530 homogeneous and nutrient supply is diffusive rather than via vascular transport – but this is not
 531 the intention. Despite the non-physiological basis of the model, however, the results display a
 532 range of behaviours and phenomena which are indicative of real tumour growth.

533 In the first instance the model is capable of reproducing homeostatic behaviour. In optimal
 534 conditions the model displays a steady turnover of cells, which age and divide in such a manner
 535 that the target cell population is preserved. However, under stress conditions, such as a
 536 restriction in the Nutrient supply or a reduction in Gene Factors, we see a change in behaviour.

537 In the case of underfeeding or starvation we see that cell numbers are markedly reduced,
538 however over-feeding does not lead to an increase in cell populations.

539 For Gene Factors, we see that under or over-supply does not impact cell numbers to the same
540 extent, though both scenarios lead to a small reduction in total cell numbers. The variations in
541 Gene Factor supply do however impact on cell turnover, with an increase in rates of cell division
542 in both under and over-supply situations. In this respect we may view the impact of deviations
543 from the Gene Factor target values acting as mitogenic factors. There is also a marked impact on
544 the calculation of cell fitness, with deviations from the optimal values fitness. We may conclude,
545 therefore, that variations in the Gene Factor supply are deleterious to some extent, but do not
546 cause the same level of cellular damage as restriction in the supply of Nutrient.

547 **Tumour Growth**

548 Once tumour growth is initiated the proliferation of cancer cells, also reflected in the number of
549 affected Grid Elements, increases in the absence of any counter-measures (i.e. left untreated). As
550 each Grid Element can support a number of cells over and above the optimum level, this initial
551 increase in numbers does not displace or replace non-cancer cells. However, once the carrying
552 capacity of the Grid Element has been reached there is a competition between cells in which
553 ultimately the Malignant cells out-compete the Normal cells. The influence of carrying capacity
554 on Malignant cell growth is illustrated in Figure 16B, which shows that changing the trigger
555 point for competition by varying the optimum cell count has an impact on the rate of tumour
556 growth. Over time the number of Malignant cells increases and the rate of invasion increases,
557 while there is a corresponding decrease in Normal cell numbers. As with the homeostatic case,
558 this behaviour is not pre-programmed but emerges from the interactions between the cells,
559 between neighbouring Grid Elements and the operation of a few simple rules. Additionally, there
560 is a consistent increase in the number of clonal sub-populations as growth continues – mirroring
561 the genetic heterogeneity which is a hall-mark of real tumour growth (Sun & Yu, 2015). The
562 system also shows that in the face of changing conditions there is an increase in the number of
563 clonal sub-populations and a decrease in the dominance of the most populous sub-clone over
564 time, again, reflecting real tumour genetic heterogeneity (Jamal-Hanjani et al., 2015).

565 We should note that in the first instance the seeded Malignant cell has the same genomic
566 structure as the Normal cell population in these experiments. That is the Malignant cell is not
567 conferred any genetic advantage over the rest of the non-Malignant cell population. The single
568 difference between the Malignant cell and the Normal cell is that the Malignant cell is flagged as
569 such and that it has an ability to mutate and undergo repeated division. In terms of Genomic
570 structure, cell Lifetime, nutrient requirements and so on there are no differences initially between
571 cell types. It may be assumed that the increasing success of the Malignant cells in outcompeting
572 Normal cells may be due to an increasing evolutionary fitness that arises through a succession of
573 mutational events occurring during cell division. However the data does not support this
574 assumption.

575 Evolutionary fitness is not defined in absolute or global terms in NEATG. Instead it is a local
576 function that reflects cellular adaption to the changing conditions *in each Grid Element*. Thus it
577 is clear from the data, as shown in Figure 4D, that in general the fitness of many Malignant cells
578 is lower than the initial fitness of the Normal cells, and that it often decreases as a result of intra-
579 Grid Element competition between cells. Furthermore, many mutations are actually deleterious
580 and do not confer evolutionary advantage over competing cells, Normal or Malignant. Some

581 Malignant cells do experience mutations which provide an advantage, and these are the cells
582 which manage to survive and expand in number. However, a cell with a positive advantage in
583 one Grid Element may migrate to an adjacent Grid Element and find that it is less fit and
584 therefore does not survive. This view of evolutionary fitness as locally responsive to the
585 environment and therefore having an impact on the success, or otherwise, of genetic mutations is
586 in line with more recent theoretical models of evolutionary processes in cancer (Rozhok &
587 DeGregori, 2015).

588 The rate of evolutionary change is initially set by the Mutation Rate, which is heritable and
589 mutable. It may be thought that the Mutation Rate would be an important driver in the rate of
590 cancer growth; however our data show that in this model it has a weak influence on the rate of
591 growth of cancer. It does however directly influence the size of the Gene Pool and the number of
592 clonal sub-populations.

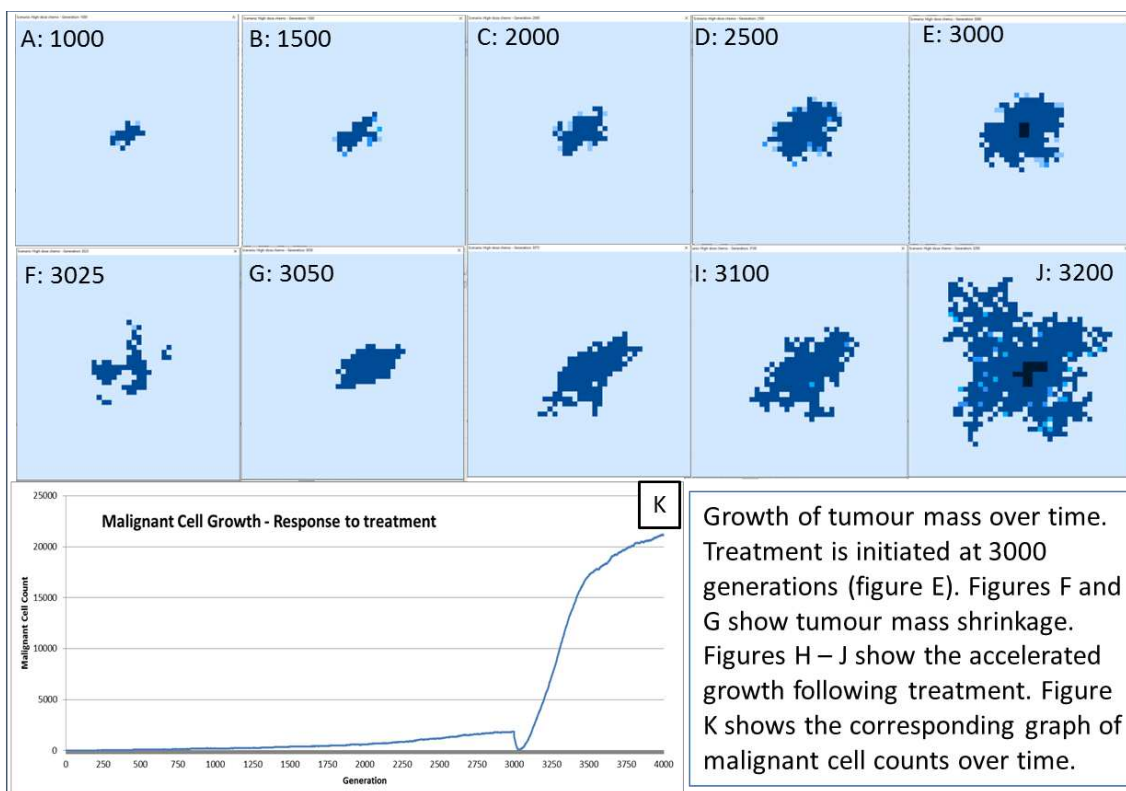
593 More influential in terms of driving growth is the Invasion Rate, which represents the probability
594 that a dividing Malignant cell in an overcrowded Grid Element can migrate to a neighbouring
595 Grid Element. The data show that this is a very strong driver of growth rates, but it does not lead
596 to the same increase in the size of the Gene Pool or the number of clonal sub-populations.

597 In terms of modelling interventions against the tumour growth we have explored the use of a
598 treatment option that loosely mimics maximum tolerated dose chemotherapy in two key respects.
599 Firstly the treatment is not genetically targeted – it applies to both Normal and Malignant cells,
600 though we can confer an increased sensitivity to Malignant cells if required. Secondly the
601 treatment induces cell death in affected cells, analogous to the apoptotic or necrotic cell death
602 induced by chemotherapy. And finally cells are affected depending on where they are in the cell
603 cycle – which is modelled in this instance by the reading of the cell clock.

604 **Tumour Regrowth**

605 One of the most interesting emergent behaviours exhibited by the NEATG system is the response
606 of the modelled tumour mass to a treatment that mimics aspects of chemotherapy treatment.

607 The response to this treatment, which we have varied in intensity and duration, is consistent in
608 our experiments. There is an initial response marked by massive tumour kill followed by a
609 resumption of tumour growth, which is often characterised by an accelerated and aggressive
610 tumour expansion, as shown in Figure 15.



611

612 **Figure 15 - Growth/Regrowth of Tumour Mass**

613 This response to treatment bears some resemblance to real cancer treatment, where an initial
 614 reduction in tumour growth, characterised as complete or partial remission, is followed by
 615 renewed tumour growth or the appearance of metastatic disease. Clinically this phenomenon is
 616 sometimes termed accelerated repopulation (Davis & Tannock, 2000; Kurtova et al., 2015; Yom,
 617 2015). While the mechanisms of treatment resistance in real tumours are complex and
 618 multifactorial it is assumed that tumour heterogeneity is an important factor; a tumour may
 619 harbour clonal subpopulations which are resistant to treatment and which therefore benefit from
 620 reduced competition after chemo-sensitive populations have been destroyed by treatment (von
 621 Manstein et al., 2013; Gottesman et al., 2016).

622 In the NEATG model treatment resistance is not related to drug efflux or other mechanisms of
 623 acquired resistance. Instead the phenomenon is associated with a pool of cells which survive due
 624 to their age (i.e. they are above the treatment cut-off age) and which are therefore faced with a
 625 decreased level of competition for resources and a lower population density of cells in each Grid
 626 Element.

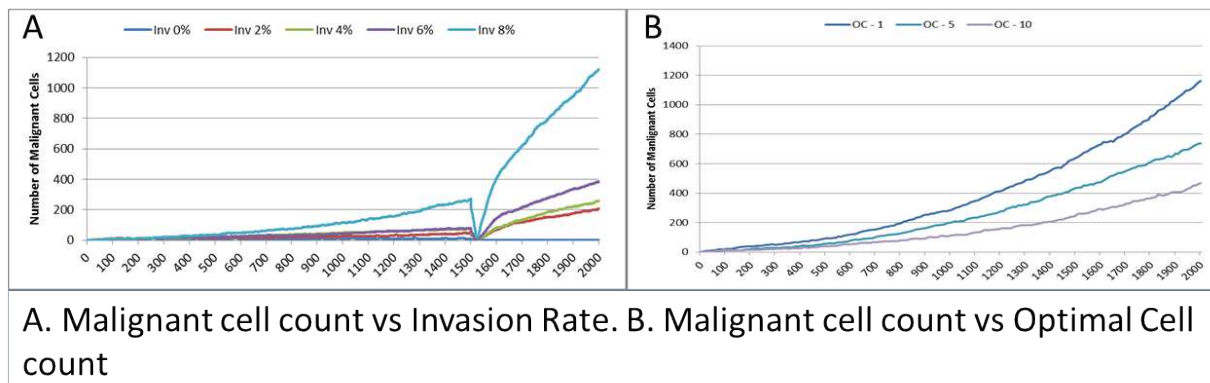
627 Increasing the intensity or duration of treatment as a strategy to improve response is shown to be
 628 problematic in that it can cause reductions in Normal cell numbers which do not recover and
 629 therefore this strategy is assumed to be deleterious. Again, there is a clear parallel to clinical
 630 experience in which increased toxicity causes excess morbidity without necessarily leading to
 631 improved outcomes.

632 **The Role of Mutations**

633 The rule of genetic mutation is a central concern in oncology, both in terms of fundamental
634 theories and increasingly at a clinical level in terms of targeted treatments. At a simplistic level
635 the SMT places the delinquent cell at the centre of cancer development, whereas the TOFT
636 places the poor neighbourhood central to the story (Baker, 2014; Sonnenschein et al., 2014). A
637 key difference between these competing theories is the role of cellular proliferation. The SMT
638 suggests that in the non-transformed state cells are non-proliferative by default. Mutations in
639 genes associated with cell cycle control mean cells become proliferative and malignant. In
640 contrast the TOFT posits that cells are proliferative by default and that this proliferative ability is
641 kept in check at the tissue level. A disordered tissue results in the removal of the proliferative
642 blocks and the cell can multiply without control.

643 In our model both cell and tissue (Grid Element) level structures are featured. The process of
644 cancer initiation consists of seeding a transformed cell into a grid element and letting it
645 proliferate. The model does not have anything to say about how the initial cell is transformed, it
646 is taken as a given. The initial cell has the same parameters as the untransformed cells, the only
647 difference is that proliferative blocks have been removed. The transformed cell, and its progeny,
648 is able to accumulate mutations during cell division and replication. Some of these mutations
649 will be deleterious and some will be advantageous, we would expect therefore that the average
650 fitness of the Malignant population will increase and that these advantageous mutations will
651 drive further evolutionary change – particularly mutations that increase the Invasion rate.
652 However this does not appear to occur. Indeed, a surprising result is that neither the Mutation
653 Rate nor the Invasion Rate, which are both heritable and mutable, appears to undergo significant
654 increase during the process of tumour growth. In fact, as shown in Figure 5B, both show
655 marginal rates of change, and can rise and fall rather than rising monotonically and driving
656 malignant growth. While some mutations may provide evolutionary advantage, it is clear that the
657 majority of mutations are passenger mutations rather than driver mutations. This is another
658 instance where the NEATG model parallels biological systems, as it has become increasingly
659 clear that the majority of somatic mutations in human tumours are also passenger mutations,
660 many of which are actively deleterious to the cancer cell (Greenman et al., 2007; McFarland et
661 al., 2013; McFarland, Mirny & Korolev, 2014).

662 The question arises then as to whether mutational change is a necessary precondition for cancer
663 growth in this model. To investigate this question an additional series of experiments was
664 performed in which the Mutation Rate was set at zero, and the Invasion Rate varied from zero to
665 8% in increments of 2%, with all other settings as in the previous set of experiments. The results
666 show that Malignant cell growth can occur even with a zero Mutation rate, which was verified by
667 confirming that the Gene Pool retained a constant value of 1 (data not shown). This may be
668 viewed as analogous to tissue hyperplasia where non-transformed cells proliferate at an increased
669 rate. The rate of growth in this model, as shown in Figure 16A, depends on the Invasion Rate, as
670 one would expect, but even at the lowest non-zero rate tumour growth occurs, and furthermore
671 the growth rate accelerates after treatment.



672

673 **Figure 16 - Invasion Rate and Optimal Cell Count**

674 What is more, the data shows that with a zero rate of Invasion and Mutation there is growth in
 675 Malignant cell numbers to the maximum possible in the Grid Element where seeding occurred,
 676 but that without an Invasion Rate there is no possibility of a Malignant cell migrating to a
 677 neighbouring Grid Element. One implication of this result is that in the NEATG model cancer
 678 growth is not driven primarily by somatic mutation and is primarily dependent on proliferation
 679 and invasiveness.

680 Reflecting on Real Tumour Growth

681 Clearly this is a very simple model that does not incorporate many biologically relevant
 682 oncogenic mechanisms – the model was deliberately designed to be as parsimonious as possible.
 683 Yet, given the limited physiology modelled by the system it has reproduced a series of emergent
 684 phenomena which are analogous to biologically relevant phenomena– tumour growth, intra-
 685 tumour genetic heterogeneity, response to virtual cytotoxic intervention and accelerated
 686 repopulation. If this thought experiment is to have any value then we must reflect on the features
 687 of the NEATG model which are responsible for these emergent behaviours and to assess whether
 688 there are corresponding physical phenomena at work in real tumour growth. Furthermore, having
 689 identified such phenomena we may generate hypotheses or look to existing evidence that suggest
 690 these phenomena are as important in real cancer as they are in the model and are therefore
 691 worthy of more focused attention from the research community.

692 By definition this is an evolutionary model, ‘descent with modification’ is a given, but as we
 693 have seen it is also possible to run the model with a zero mutation rate and still generate a
 694 growing population of Malignant cells. One notes that although they harbour no mutations and
 695 may be considered Normal cells with a hyperplastic phenotype, there are also rare instances of
 696 cancers in which no genetic mutations or epigenetic drivers are present (Versteeg, 2014). We
 697 have also defined Malignant cells as those with the ability to mutate and to move into
 698 neighbouring Grid Elements. How these abilities arise is not a question we are investigating in
 699 the model. What then are the key drivers of tumour growth and accelerated repopulation? The
 700 detailed analysis of the behaviours outlined in the Results suggests that there are two key drivers:

- 701 • Cell competition
- 702 • Cell death

703

704 Competition occurs in the NEATG model within each Grid Element when the population density
705 reaches a set level (the optimum cell count). As can be seen in Figure 16B, when competition
706 begins earlier (when the optimum cell count is 1), the rate of tumour growth is much higher. As
707 one would expect, competition also spurs growth of the gene pool (data not shown). Competition
708 for resources leads to cell death when the number of cells exceeds the carrying capacity of the
709 Grid Element. A ranked selection algorithm means that the least fit (within that Grid Element)
710 cells are removed. Importantly, this competitive process takes place entirely within a Grid
711 Element and is a process that involves both cell-to-cell (cell-autonomous) and tissue-level (non-
712 cell-autonomous, defined by the optimum cell count for the Grid Element) factors.

713 Cell death arises both from the competition between cells within each Grid Element and also
714 exogenously via ‘treatment’ – in this work loosely modelled on maximum tolerated dose
715 chemotherapy. It is clear from the data that increasing the rate of cell death, both in Normal and
716 Malignant cells, leads to accelerated repopulation and more aggressive tumour growth.

717 Many of the *core* findings from molecular biology are *not* included in this model. For example
718 the NEATG model does not explicitly make use of the cancer stem cell hypothesis. Cancer stem
719 cells (CSC), also known as tumour-initiating or cancer-initiating cells, are functionally
720 characterised as a small fraction of tumour cell populations with the ability to self-renew,
721 differentiate into multiple cell types and to generate new tumours when transplanted (Reya et al.,
722 2001; Jordan, Guzman & Noble, 2006; Bozorgi, Khazaei & Khazaei, 2015). Crucially, CSC are
723 assumed to generate the non-CSC cells which make up the major population of malignant cells
724 in a tumour. In addition to being characterised by a range of cell markers (CD44+, CD133+,
725 ALDH1 etc), CSC are theorised to be relatively chemo- and radio-resistant and a key factor in
726 resistance to treatment (Yang & Rycaj, 2015).

727 However, the CSC hypothesis is increasingly being challenged as evidence emerges that rather
728 than being a distinct cell population there is a set of properties which together define ‘stemness’
729 (Lewis, 2008; Antoniou et al., 2013; Wang et al., 2015). In particular the claim that tumour
730 growth is mainly attributable to the rapid proliferation of CSC populations rather than the non-
731 CSC fraction is open to some dispute (Adams & Strasser, 2008; Hegde et al., 2012). Additionally
732 there is evidence that cancer cells display a significant degree of plasticity such that ‘stemness’
733 traits can be acquired by non-CSC cells (Chaffer et al., 2011; Cabrera, Hollingsworth & Hurt,
734 2015). Indeed some recent work suggests that non-CSC cells acquire stem-like properties in
735 response to therapeutic challenge with chemotherapy (Hu et al., 2012; Martins-Neves et al.,
736 2016).

737 NEATG, therefore, does not explicitly model CSC and non-CSC populations but makes the
738 simplifying assumption that all Malignant cells are proliferative. The key point is that the
739 existence of CSC, whether as a separate population of cells or a collection of cellular traits, is
740 immaterial to the operation of the model and the ability to reproduce tumour cell growth. At this
741 level of abstraction the behaviour of the model would be the same regardless of the underlying
742 complexities of the CSC hypothesis.

743 Similarly the model does not include oncogenes, specific molecular pathways, a realistic cell
744 cycle, a vascular or lymphatic system, immune responses, different cell types, tumour stroma and
745 many more biologically important aspects of real disease. However, the model does propose that
746 cell competition and cell death have an important, and perhaps underestimated, role in patterns of

747 tumour growth and response to treatment. Given that induction of cell death, particularly via the
748 apoptotic pathway, is central to the most common forms of cancer treatment this would be of
749 some clinical significance if confirmed in the laboratory.

750 There are some indications that these two aspects of cancer biology are of biological
751 significance.

752 A number of investigators have looked at the question of the role of cell competition in cancer,
753 for example Baker and Li (Baker & Li, 2008), and Moreno (Moreno, 2008), both referring to
754 results from research in *Drosophila melanogaster* which outlined the process whereby cells of
755 differing genotype *within* a given compartment engage in competition such that *locally* less fit
756 cells undergo apoptosis and are replaced with *locally* fitter cells. Very recent work by
757 Suijkerbuijk et al has described the process whereby cell competition between APC^{-/-} intestinal
758 adenoma cells and normal host cells in *Drosophila melanogaster* leads to cell death in normal
759 cells, host tissue attrition and the invasion of more rapidly proliferating adenoma cells
760 (Suijkerbuijk et al., 2016). Eichenlaub and colleagues have also investigated cell competition in
761 the same animal model (Eichenlaub, Cohen & Herranz, 2016). They report that EGFR over-
762 expression in wing imaginal disc cells leads to benign tissue hyperplasia and subsequent
763 epithelial tumour formation.

764 We should note that there are different cell types, molecular drivers and pathways active in the
765 latter two studies, yet both groups report that blocking the apoptotic process blocks tumour
766 development. This prompts the conclusion that targeting cell competition itself may be a valid
767 strategy in cancer therapy (Gil & Rodriguez, 2016).

768 While cell competition may be a necessary pre-condition of cancer development, it is not
769 sufficient, and our model clearly indicates that cell death is also required. This poses the question
770 as to the role of cell death, particularly apoptosis, in tumour growth. One of the hallmarks of
771 cancer is defined as ‘resistance to apoptosis’ (Hanahan & Weinberg, 2011), yet it is known that
772 tumours show a high rate of apoptosis, and at least in some cancer types high apoptosis rates are
773 a negative prognostic factor (Nishimura et al., 1999). A number of recent studies have outlined
774 the much more complex relationship between cancer and apoptosis than has been assumed in the
775 past (Gregory & Pound, 2011; Wang et al., 2013; Labi & Erlacher, 2015; Lauber & Herrmann,
776 2015; Ford et al., 2015). While these studies outline numerous mechanistic explanations as to
777 why increased apoptosis may lead to increased tumour growth, it is clear that there are
778 underlying phenomena which may have important clinical implications in terms of treatment
779 strategies.

780 One rather obvious conclusion is that rather than aiming at maximum tumour kill using
781 traditional cytotoxic chemotherapy perhaps, other treatment strategies which produce lower
782 levels of cancer cell death may be more beneficial. For example, using metronomic
783 chemotherapy, in which chemotherapeutic drugs are administered at non-cytotoxic doses and
784 with no treatment breaks is one such strategy (Scharovsky, Mainetti & Rozados, 2009; Kareva,
785 Waxman & Klement, 2014; André, Carré & Pasquier, 2014). Another example is the concept of
786 ‘adaptive therapy’, in which chemotherapy is used to maintain a population of tumour cells
787 rather than aiming to maximise tumour kill (Gatenby et al., 2009; Enriquez-Navas et al., 2016).

788 While it is clear that the NEATG system does not provide us with mechanistic explanations for
789 the pro-tumour growth effects of cell competition and apoptosis, it does direct our attention to
790 these areas of current, active but not yet mainstream research. Starting from a simplified and non-
791 physiological model of cell and tissue level interactions our results reproduce relevant biology-
792 like behaviour and provides us with some indications of the key drivers involved. In turn if we
793 view this as the result of a thought experiment we can reflect on real systems and derive
794 hypotheses about areas of relevant research. Having directed our attention to the role of cell
795 competition and cell death there is ample scope for continuing to use the model to explore the
796 processes at work and, perhaps, to suggest relevant laboratory experiments in light of further
797 model results.

798 **Conclusion**

799 There is scope, of course, for improving the model in a number of ways without necessarily
800 abandoning the non-physiological basis of it. Having identified cell competition and apoptosis as
801 key concerns we may look to incorporate additional aspects of this in more detail. For example
802 the onset of cell competition is triggered when the optimum cell count is reached. In part this is a
803 function of the carrying capacity of the Grid Element – when this level is exceeded Malignant
804 cells are able to migrate to a randomly selected neighbouring Grid Element (a stochastic process
805 depending on the Invasion Rate). In some respects this is analogous to tissue stiffness or rigidity
806 in that Grid Elements can be made more or less ‘stiff’ by increasing or decreasing the carrying
807 capacity. Tissue stiffness is also a current concern in oncology (Wei & Yang, 2016) that may be
808 amenable to additional thought experimentation by extending this model.

809 NEATG has been designed as a platform for investigating different interventions and how they
810 impact the growth of Malignant cells and tumour Grid Elements. In the experiments described in
811 this paper only one strategy, loosely based on maximum tolerated dose chemotherapy, has been
812 explored. Clearly there is scope for additional interventions to be modelled, for example
813 combinations of Nutrient restriction and chemotherapy, a treatment strategy of some clinical
814 interest (Raffaghello et al., 2008; Safdie et al., 2009; Lee et al., 2012), may be modelled in
815 NEATG. Similarly the use of metronomic chemotherapy, chemo-switch strategies, targeted
816 therapies and the use of different treatment schedules are also amenable to modelling using the
817 NEATG system.

818 The value of agent-based evolutionary models is that they can generate biologically relevant
819 behaviour through algorithmic means, which may in turn shed new light on the underlying
820 biological systems. Obviously increasing the complexity of the model so that additional features
821 are included may be of some value. However, the success of a thought experiment lies as much
822 in the detail of what features of reality are excluded – a process that removes many physiological
823 details from the model – as it does on what features are included. In this case the model has
824 raised questions as to the role that cell competition and cell death have in cancer, suggesting that
825 these relatively under-researched processes may have much greater importance than has hitherto
826 been accepted.

827

828 **References**

- 829 Adams JM., Strasser A. 2008. Is tumor growth sustained by rare cancer stem cells or dominant clones?
830 *Cancer research* 68:4018–21.
- 831 Allen M., Louise Jones J. 2011. Jekyll and Hyde: the role of the microenvironment on the progression of
832 cancer. *The Journal of pathology* 223:162–76.
- 833 André N., Carré M., Pasquier E. 2014. Metronomics: towards personalized chemotherapy? *Nature*
834 *reviews. Clinical oncology* 11:413–31.
- 835 Antoniou A., Hébrant A., Dom G., Dumont JE., Maenhaut C. 2013. Cancer stem cells, a fuzzy evolving
836 concept: a cell population or a cell property? *Cell cycle (Georgetown, Tex.)* 12:3743–8.
- 837 Baker SG. 2014. A Cancer Theory Kerfuffle Can Lead to New Lines of Research. *JNCI Journal of the*
838 *National Cancer Institute* 107:dju405–dju405.
- 839 Baker NE., Li W. 2008. Cell competition and its possible relation to cancer. *Cancer Research* 68:5505–
840 5507.
- 841 Barcellos-Hoff MH., Lyden D., Wang TC. 2013. The evolution of the cancer niche during multistage
842 carcinogenesis. *Nature reviews. Cancer* 13:511–8.
- 843 Basanta D., Simon M., Hatzikirou H., Deutsch a. 2008. Evolutionary game theory elucidates the role of
844 glycolysis in glioma progression and invasion. *Cell Proliferation* 41:980–987.
- 845 Bizzarri M., Cucina A. 2014. Tumor and the microenvironment: a chance to reframe the paradigm of
846 carcinogenesis? *BioMed research international* 2014:934038.
- 847 Bozorgi A., Khazaei M., Khazaei MR. 2015. New Findings on Breast Cancer Stem Cells: A Review. *Journal*
848 *of breast cancer* 18:303–12.
- 849 Cabrera MC., Hollingsworth RE., Hurt EM. 2015. Cancer stem cell plasticity and tumor hierarchy. *World*
850 *journal of stem cells* 7:27–36.
- 851 Chaffer CL., Brueckmann I., Scheel C., Kaestli AJ., Wiggins PA., Rodrigues LO., Brooks M., Reinhardt F., Su
852 Y., Polyak K., Arendt LM., Kuperwasser C., Bieri B., Weinberg RA. 2011. Normal and neoplastic
853 nonstem cells can spontaneously convert to a stem-like state. *Proceedings of the National*
854 *Academy of Sciences of the United States of America* 108:7950–5.
- 855 Chen Y., Jungsuwadee P., Vore M., Butterfield DA., St Clair DK. 2007. Collateral damage in cancer
856 chemotherapy: oxidative stress in nontargeted tissues. *Molecular interventions* 7:147–56.
- 857 Davis a J., Tannock JF. 2000. Repopulation of tumour cells between cycles of chemotherapy: a neglected
858 factor. *The Lancet. Oncology* 1:86–93.
- 859 Eichenlaub T., Cohen SM., Herranz H. 2016. Cell Competition Drives the Formation of Metastatic Tumors
860 in a Drosophila Model of Epithelial Tumor Formation. *Current biology : CB* 26:419–27.
- 861 Enderling H., Hahnfeldt P. 2011. Cancer stem cells in solid tumors: is “evading apoptosis” a hallmark of
862 cancer? *Progress in biophysics and molecular biology* 106:391–9.
- 863 Enderling H., Hlatky L., Hahnfeldt P. 2009. Migration rules: tumours are conglomerates of self-
864 metastases. *British journal of cancer* 100:1917–1925.
- 865 Enriquez-Navas PM., Kam Y., Das T., Hassan S., Silva A., Foroutan P., Ruiz E., Martinez G., Minton S.,
866 Gillies RJ., Gatenby RA. 2016. Exploiting evolutionary principles to prolong tumor control in

- 867 preclinical models of breast cancer. *Science translational medicine* 8:327ra24.
- 868 Fisher R., Pusztai L., Swanton C. 2013. Cancer heterogeneity: implications for targeted therapeutics.
869 *British journal of cancer* 108:479–85.
- 870 Ford CA., Petrova S., Pound JD., Voss JLP., Melville L., Paterson M., Farnworth SL., Gallimore AM., Cuff
871 S., Wheadon H., Dobbin E., Ogden CA., Dumitriu IE., Dunbar DR., Murray PG., Ruckerl D., Allen JE.,
872 Hume DA., van Rooijen N., Goodlad JR., Freeman TC., Gregory CD. 2015. Oncogenic properties of
873 apoptotic tumor cells in aggressive B cell lymphoma. *Current biology : CB* 25:577–88.
- 874 Gatenby RA., Silva AS., Gillies RJ., Frieden BR. 2009. Adaptive therapy. *Cancer research* 69:4894–903.
- 875 Gatenby RA., Gillies RJ., Brown JS. 2011. Of cancer and cave fish. *Nature reviews. Cancer* 11:237–238.
- 876 Gerlee P., Anderson ARA. 2007. An evolutionary hybrid cellular automaton model of solid tumour
877 growth. *Journal of theoretical biology* 246:583–603.
- 878 Gerlee P., Basanta D., Anderson ARA. 2011. Evolving homeostatic tissue using genetic algorithms.
879 *Progress in biophysics and molecular biology* 106:414–25.
- 880 Gil J., Rodriguez T. 2016. Cancer: The Transforming Power of Cell Competition. *Current biology : CB*
881 26:R164–6.
- 882 Gillies RJ., Verduzco D., Gatenby R a. 2012. Evolutionary dynamics of carcinogenesis and why targeted
883 therapy does not work. *Nature reviews. Cancer* 12:487–493.
- 884 Gottesman MM., Lavi O., Hall MD., Gillet J-P. 2016. Toward a Better Understanding of the Complexity of
885 Cancer Drug Resistance. *Annual review of pharmacology and toxicology* 56:85–102.
- 886 Greenman C., Stephens P., Smith R., Dalgliesh GL., Hunter C., Bignell G., Davies H., Teague J., Butler A.,
887 Stevens C., Edkins S., O'Meara S., Vastrik I., Schmidt EE., Avis T., Barthorpe S., Bhamra G., Buck G.,
888 Choudhury B., Clements J., Cole J., Dicks E., Forbes S., Gray K., Halliday K., Harrison R., Hills K.,
889 Hinton J., Jenkinson A., Jones D., Menzies A., Mironenko T., Perry J., Raine K., Richardson D.,
890 Shepherd R., Small A., Tofts C., Varian J., Webb T., West S., Widaa S., Yates A., Cahill DP., Louis DN.,
891 Goldstraw P., Nicholson AG., Brasseur F., Looijenga L., Weber BL., Chiew Y-E., DeFazio A., Greaves
892 MF., Green AR., Campbell P., Birney E., Easton DF., Chenevix-Trench G., Tan M-H., Khoo SK., Teh
893 BT., Yuen ST., Leung SY., Wooster R., Futreal PA., Stratton MR. 2007. Patterns of somatic mutation
894 in human cancer genomes. *Nature* 446:153–158.
- 895 Gregory CD., Pound JD. 2011. Cell death in the neighbourhood: direct microenvironmental effects of
896 apoptosis in normal and neoplastic tissues. *The Journal of pathology* 223:177–94.
- 897 Hanahan D., Coussens LM. 2012. Accessories to the Crime: Functions of Cells Recruited to the Tumor
898 Microenvironment. *Cancer Cell* 21:309–322.
- 899 Hanahan D., Weinberg RA. 2011. Hallmarks of cancer: the next generation. *Cell* 144:646–74.
- 900 Hegde G V., de la Cruz C., Eastham-Anderson J., Zheng Y., Sweet-Cordero EA., Jackson EL. 2012. Residual
901 tumor cells that drive disease relapse after chemotherapy do not have enhanced tumor initiating
902 capacity. *PLoS one* 7:e45647.
- 903 Hu X., Ghisolfi L., Keates AC., Zhang J., Xiang S., Lee D., Li CJ. 2012. Induction of cancer cell stemness by
904 chemotherapy. *Cell cycle (Georgetown, Tex.)* 11:2691–8.
- 905 Jalali R., Mitra I., Badwe R. 2016. Cancer research: in need of introspection. *The Lancet. Oncology*

- 906 17:140–1.
- 907 Jamal-Hanjani M., Quezada SA., Larkin J., Swanton C. 2015. Translational Implications of Tumor
908 Heterogeneity. *Clinical Cancer Research* 21:1258–1266.
- 909 Janes K a., Lauffenburger D a. 2013. Models of signalling networks - what cell biologists can gain from
910 them and give to them. *Journal of cell science* 126:1913–21.
- 911 Jordan CT., Guzman ML., Noble M. 2006. Cancer stem cells. *The New England journal of medicine*
912 355:1253–61.
- 913 Kareva I. 2011. What can ecology teach us about cancer? *Translational oncology* 4:266–70.
- 914 Kareva I., Waxman DJ., Klement GL. 2014. Metronomic chemotherapy: An attractive alternative to
915 maximum tolerated dose therapy that can activate anti-tumor immunity and minimize therapeutic
916 resistance. *Cancer letters* 358:14–17.
- 917 Krzeslak M., Swierniak A. 2014. Four Phenotype Model of Interaction Between Tumour Cells. In: *World*
918 *Congress*. 11536–11541.
- 919 Kurtova A V., Xiao J., Mo Q., Pazhanisamy S., Krasnow R., Lerner SP., Chen F., Roh TT., Lay E., Ho PL.,
920 Chan KS. 2015. Blocking PGE2-induced tumour repopulation abrogates bladder cancer
921 chemoresistance. *Nature* 517:209–13.
- 922 Labi V., Erlacher M. 2015. How cell death shapes cancer. *Cell death & disease* 6:e1675.
- 923 Lauber K., Herrmann M. 2015. Tumor Biology: With a Little Help from My Dying Friends. *Current Biology*
924 25:R198–R201.
- 925 Lee C., Raffaghello L., Brandhorst S., Safdie FM., Bianchi G., Martin-Montalvo A., Pistoia V., Wei M.,
926 Hwang S., Merlino A., Emionite L., de Cabo R., Longo VD. 2012. Fasting cycles retard growth of
927 tumors and sensitize a range of cancer cell types to chemotherapy. *Science translational medicine*
928 4:124ra27.
- 929 Lewis MT. 2008. Faith, heresy and the cancer stem cell hypothesis. *Future oncology (London, England)*
930 4:585–9.
- 931 von Manstein V., Yang CM., Richter D., Delis N., Vafaizadeh V., Groner B. 2013. Resistance of Cancer
932 Cells to Targeted Therapies Through the Activation of Compensating Signaling Loops. *Current signal*
933 *transduction therapy* 8:193–202.
- 934 Martins-Neves SR., Paiva-Oliveira DI., Wijers-Koster PM., Abrunhosa AJ., Fontes-Ribeiro C., Bovée JVMG.,
935 Cleton-Jansen A-M., Gomes CMF. 2016. Chemotherapy induces stemness in osteosarcoma cells
936 through activation of Wnt/ β -catenin signaling. *Cancer letters* 370:286–95.
- 937 McFarland CD., Korolev KS., Kryukov G V., Sunyaev SR., Mirny L a. 2013. Impact of deleterious passenger
938 mutations on cancer progression. *Proceedings of the National Academy of Sciences* 110:2910–
939 2915.
- 940 McFarland CD., Mirny LA., Korolev KS. 2014. Tug-of-war between driver and passenger mutations in
941 cancer and other adaptive processes. *Proceedings of the National Academy of Sciences* 111:15138–
942 15143.
- 943 Moreno E. 2008. Is cell competition relevant to cancer? *Nature reviews. Cancer* 8:141–147.
- 944 Nishimura R., Nagao K., Miyayama H., Matsuda M., Baba K., Matsuoka Y., Yamashita H., Fukuda M.,

- 945 Higuchi A. 1999. Apoptosis in breast cancer and its relationship to clinicopathological
946 characteristics and prognosis. *Journal of surgical oncology* 71:226–34.
- 947 Pantziarka P. 2015. Primed for cancer: Li Fraumeni Syndrome and the pre-cancerous niche.
948 *Ecancermedicalscience* 9:541.
- 949 Paolo D., Ezequiel A., Noble J., Bullock S. 2000. Simulation models as opaque thought experiments.
950 *Artificial Life VII The Seventh International Conference on the Simulation and Synthesis of Living*
951 *Systems*:497–506.
- 952 Poleszczuk J., Enderling H. 2016. Cancer Stem Cell Plasticity as Tumor Growth Promoter and Catalyst of
953 Population Collapse. *Stem cells international* 2016:3923527.
- 954 Psaila B., Kaplan RN., Port ER., Lyden D. 2007. Priming the “soil” for breast cancer metastasis: the pre-
955 metastatic niche. *Breast disease* 26:65–74.
- 956 Quail DF., Joyce J a. 2013. Microenvironmental regulation of tumor progression and metastasis. *Nature*
957 *medicine* 19:1423–37.
- 958 Raffaghello L., Lee C., Safdie FM., Wei M., Madia F., Bianchi G., Longo VD. 2008. Starvation-dependent
959 differential stress resistance protects normal but not cancer cells against high-dose chemotherapy.
960 *Proceedings of the National Academy of Sciences of the United States of America* 105:8215–20.
- 961 Reya T., Morrison SJ., Clarke MF., Weissman IL. 2001. Stem cells, cancer, and cancer stem cells. *Nature*
962 414:105–11.
- 963 Ribba B., Alarcon T., Marron K., Maini PK., Agur Z. 2004. *Cellular Automata*. Berlin, Heidelberg: Springer
964 Berlin Heidelberg.
- 965 Rozhok AI., DeGregori J. 2015. Toward an evolutionary model of cancer: Considering the mechanisms
966 that govern the fate of somatic mutations. *Proceedings of the National Academy of Sciences of the*
967 *United States of America* 112:8914–8921.
- 968 Saetzler K., Sonnenschein C., Soto AM. 2011. Systems biology beyond networks: Generating order from
969 disorder through self-organization. *Seminars in Cancer Biology* 21:165–174.
- 970 Safdie FM., Dorff T., Quinn D., Fontana L., Wei M., Lee C., Cohen P., Longo VD. 2009. Fasting and cancer
971 treatment in humans: A case series report. *Aging* 1:988–1007.
- 972 Scharovsky OG., Mainetti LE., Rozados VR. 2009. Metronomic chemotherapy: changing the paradigm
973 that more is better. *Current oncology (Toronto, Ont.)* 16:7–15.
- 974 Silva AS., Gatenby R a. 2010. A theoretical quantitative model for evolution of cancer chemotherapy
975 resistance. *Biology direct* 5:25.
- 976 Sonnenschein C., Soto AM., Rangarajan A., Kulkarni P. 2014. Competing views on cancer. *Journal of*
977 *biosciences* 39:281–302.
- 978 De Sousa E Melo F., Vermeulen L., Fessler E., Medema JP. 2013. Cancer heterogeneity--a multifaceted
979 view. *EMBO reports* 14:686–95.
- 980 Suijkerbuijk SJE., Kolahgar G., Kucinski I., Piddini E. 2016. Cell Competition Drives the Growth of
981 Intestinal Adenomas in Drosophila. *Current biology : CB* 26:428–38.
- 982 Sun X., Yu Q. 2015. Intra-tumor heterogeneity of cancer cells and its implications for cancer treatment.
983 *Acta pharmacologica Sinica* 36:1219–27.

- 984 Tian T., Olson S., Whitacre JM., Harding A. 2011. The origins of cancer robustness and evolvability.
985 *Integrative biology : quantitative biosciences from nano to macro* 3:17–30.
- 986 Versteeg R. 2014. Cancer: Tumours outside the mutation box. *Nature* 506:438–9.
- 987 Wang R-A., Li Q-L., Li Z-S., Zheng P-J., Zhang H-Z., Huang X-F., Chi S-M., Yang A-G., Cui R. 2013. Apoptosis
988 drives cancer cells proliferate and metastasize. *Journal of cellular and molecular medicine* 17:205–
989 11.
- 990 Wang T., Shigdar S., Gantier MP., Hou Y., Wang L., Li Y., Al Shamaileh H., Yin W., Zhou S., Zhao X., Duan
991 W. 2015. Cancer stem cell targeted therapy: progress amid controversies. *Oncotarget* 6.
- 992 Wei SC., Yang J. 2016. Forcing through Tumor Metastasis: The Interplay between Tissue Rigidity and
993 Epithelial-Mesenchymal Transition. *Trends in cell biology* 26:111–20.
- 994 Weinberg RA. 2014. Coming full circle - From endless complexity to simplicity and back again. *Cell*
995 157:267–271.
- 996 Yang T., Rycaj K. 2015. Targeted therapy against cancer stem cells. *Oncology letters* 10:27–33.
- 997 Yom SS. 2015. Accelerated repopulation as a cause of radiation treatment failure in non-small cell lung
998 cancer: review of current data and future clinical strategies. *Seminars in radiation oncology* 25:93–
999 9.
- 1000
- 1001